Expert Systems With Applications 287 (2025) 127917

Contents lists available at ScienceDirect

Expert Systems With Applications

journal homepage: www.elsevier.com/locate/eswa

Decentralized multipartite consensus model for multi-attribute group decision making: A user experience-oriented perspective

Ya-Jing Zhou [a,b], Mi Zhou [a,b,*], Jian-Bo Yang [c], Ba-Yi Cheng [a,b], Jian Wu [d]

[a] School of Management, Hefei University of Technology, Hefei, Anhui 230009, China
[b] Ministry of Education Engineering Research Centre for Intelligent Decision-Making & Information System Technologies, Hefei, Anhui 230009, China
[c] Alliance Manchester Business School, The University of Manchester, M15 6PB, UK
[d] School of Economics and Management, Shanghai Maritime University, Shanghai 201306, China

ARTICLE INFO

Keywords:
User experience-oriented attribute system
Multi-granularity preference
Decentralized multipartite feedback mechanism
Opinion fusion
Consensus reaching process

ABSTRACT

In multi-attribute group decision making (MAGDM), capturing user preferences and accurately building consensus among different stakeholders is critical. This paper introduces a new data-driven framework that utilizes user-generated content (UGC) to extract and refine user experience systematically attributes to improve decision accuracy. This user experience-oriented attribute system generation method involves the implementation of text mining and natural language processing. This system efficiently processes large-scale data, optimizing attribute discovery and aggregation to represent user preferences accurately. Furthermore, an Interest-Expertise matrix is proposed that classifies decision-makers (DMs) based on their interests and expertise. A novel pairwise comparison method as a multi-granularity distributed preference relation (DPR) is developed to align decision granularity with their capabilities. A decentralized multipartite feedback mechanism caters to varied stakeholder groups, facilitating a robust consensus reaching process (CRP). Different optimal models are designed for corresponding decision-making participants in this mechanism. A case study for selecting the optimal research and development (R&D) alternative for a new energy vehicle (NEV) company is presented to demonstrate the application of our framework in a realistic scenario, highlighting its effectiveness in enhancing strategic decision-making processes within the organization. This study contributes to the field of MAGDM by providing a fusion-based approach to integrate user-centric data into organizational decision-making frameworks, aiming for more targeted and effective outcomes.

1. Introduction

Multi-attribute group decision making (MAGDM) is an essential methodology within decision science, facilitating the evaluation and prioritization of options across various fields, from government (Liu et al., 2023; Ma et al., 2020), engineering (Kumar & Chen, 2022; Xing et al., 2022), medical (Tang et al., 2023b) to business (Tang et al., 2023a; Wu et al., 2022; Xue et al., 2021) management. This method allows for systematic decision-making by considering multiple attributes simultaneously, which is crucial in scenarios where complex, multi-faceted challenges need balanced solutions (Bai et al., 2024). The complexity of MAGDM stems from the need to accommodate diverse preferences among multiple decision makers (DMs) and the necessity to consider a wide array of attributes. Traditional approaches often fall short of capturing the full spectrum of user preferences, which leads to decisions that are less than ideal. Therefore, leveraging data-driven and knowledge-based analytics to enhance the robustness and accuracy of decision models is a key challenge in research. However, rapid changes in technology and consumer behaviors require MAGDM approaches that continuously adapt to evolving markets. Static attribute systems may overlook valuable emerging data, especially user-generated content (UGC), limiting decision quality and relevance.

With the rapid development of the new generation of information technology, the decision environment is becoming increasingly dynamic and complex. Traditional MAGDM approaches, which often rely on the same set of predefined attributes (Dong et al., 2016; Liu et al., 2023; Ma et al., 2020), may not reflect real-time decision environments or evolving market dynamics. In contrast, inspired by data-driven decision

* Corresponding author at: School of Management, Hefei University of Technology, Hefei, Anhui 230009, China.
E-mail addresses: zhouyj@mail.hfut.edu.cn (Y.-J. Zhou), zhoumi@hfut.edu.cn (M. Zhou), jian-bo.yang@manchester.ac.uk (J.-B. Yang), chengbayi@hfut.edu.cn (B.-Y. Cheng), jwu@shmtu.edu.cn (J. Wu).

https://doi.org/10.1016/j.eswa.2025.127917
Received 13 October 2024; Received in revised form 21 February 2025; Accepted 25 April 2025
Available online 30 April 2025
0957-4174/

making analytics method, user-generated content (UGC) offers a dynamic and continuously updated source of data that can better capture consumer preferences and trends (Liu et al., 2023). It includes online reviews (He et al., 2022), social media (Liu et al., 2023), and user feedback (Ji et al., 2023a), which directly informs MAGDM models by incorporating real-time consumer sentiments into attribute generation. It provides direct insights into consumer behaviors and preferences, making it a valuable resource for tailoring products and services to meet user demands. Therefore, integrating UGC into MAGDM using data-driven methods to generate user experience-oriented (UXO) attribute sets is a crucial challenge.

DM's preference expression scheme is another crucial problem based on the constructed attribute set. In the realm of MAGDM, the preference schemes given by DMs may be homogeneous or heterogeneous. The former often entails the uniform evaluation of attributes using a consistent format (Zhou et al., 2022a; Zhou et al., 2024), whereas the latter allows for the use of diverse preference schemes such as real numbers, interval values, fuzzy numbers, and linguistic term sets (LTS) due to the complexity and variability of decision scenarios (Tang et al., 2019; B. Zhang, Liang, Zhang, & Xu, 2018; H. Zhang, Dong, & Herrera-Viedma, 2018). These schemes have evolved to handle both homogeneous and heterogeneous preferences effectively within MAGDM frameworks. However, a significant challenge remains in accommodating the varying information granularity perceptions of DMs (Tang et al., 2022; Wang and Liang, 2020; Zhang et al., 2021). Despite using the same preference expression method with a pairwise comparison structure (Fu et al., 2019; Zhang et al., 2016), DMs may perceive and express decision attributes differently due to their diverse expertise backgrounds. This variation in information granularity can significantly impact the evaluation system or rating scales. Therefore, handling the diverse granularity perceptions in DM's preference expression remains challenging in MAGDM.

Consensus reaching process (CRP) in MAGDM has evolved to address the complex dynamic situations (Li et al., 2022; Zhou et al., 2022c) and conflicting stakeholder groups (Xu et al., 2015). While traditional models strive for unanimous decisions, it is impractical and inefficient in real-world scenarios, where speed and adaptability are crucial (Bezdek et al., 1978). As a result, soft consensus models that provide dynamic feedback mechanisms have become prevalent (Chen et al., 2024; Wei et al., 2023). This mechanism suggests modifications to DMs' opinions, facilitating a balance between achieving consensus and maintaining decision-making efficiency. Moreover, the development of feedback strategies has further refined the CRP. This strategy effectively bridges the gap between opinion adjustment and social relationships, enhancing the decision-making framework's capability to handle complex decisions (Guo et al., 2020; Zhang et al., 2022; Zhou et al., 2023). Recent advancements include the identification rule and direction rule-based feedback mechanism (Tang et al., 2019) and optimization rule-based feedback mechanism (Cheng et al., 2020; Han et al., 2022; Tang et al., 2025). A critical challenge is to accommodate the diverse interests of stakeholders with organizational goals. Moreover, incorporating heterogeneous stakeholder interests into a unified MAGDM framework remains non-trivial. Diverse expertise levels can lead to conflicting objectives, and insufficient attention to these variations can undermine consensus stability and decision quality.

The following outlines the gaps identified in developing consensus models for MAGDM based on UGC:

1) Typically, the attribute systems for MAGDM are derived from predefined standards or literature, which may not capture real-time UGC updates. There is a need for a system that integrates and continually updates UGC features, ensuring they are up-to-date and reflective of actual user experience.

2) Current models typically use a uniform approach to express DM's preference, neglecting the diversity in their expertise. A more flexible model that can adapt to the expertise levels of DMs, allowing for generalized and specialized inputs, is crucial for more effective decision-making.

3) While existing consensus models consider DM behavior, they often overlook the comprehensive inclusion of diverse stakeholder perspectives, particularly in scenarios with conflicting interests. There is a gap in models that systematically integrate and balance these diverse interests to reach a robust consensus.

Hence, this research aims to develop a decentralized multipartite consensus model for MAGDM that explicitly leverages UGC-driven, real-time attribute generation and adapts to varying DM expertise. By addressing the above gaps, we seek to enhance the accuracy and practicality of modern decision-making frameworks. The following main contributions are briefly summarized as follows:

1) A UXO attribute system is developed, leveraging a data-driven approach focused on UGC. Advanced data acquisition and Sentence-BERT (SBERT) are utilized with segment soft relative cosine similarity (SSRcos) to enhance semantic comparison accuracy in large-scale corpora. Dimensionality reduction through Uniform Manifold Approximation and Projection (UMAP)-assisted Hierarchical Density-Based Spatial Clustering of Applications with Noise (HDBSCAN) is employed, followed by attribute integration using attribute-based Term Frequency–Inverse Document Frequency (A-TF-IDF).

2) An Interest-Expertise (I-E) matrix tailored for MAGDM is introduced. This novel decision mechanism for MAGDM uses I-E matrix to classify DMs by interests and domain expertise. It aligns decision granularity with DMs' capabilities, customizes processes for expert and non-expert stakeholders, and enhances decision quality and engagement within organizational frameworks.

3) A decentralized multipartite feedback consensus mechanism is designed within the MAGDM framework. It assesses internal consensus levels among diverse stakeholder entities and categorizes them into decision-making participative parties. This process aligns stakeholder feedback with multi-objective optimization models, fostering comprehensive and inclusive consensus across varied entities.

The rest of this paper is organized as follows: Section 2 gives the framework of the proposed approach and provides necessary preliminaries. Section 3 discusses the procedure for generating a UXO attribute system. Section 4 introduces a decentralized multipartite consensus mechanism tailored for MAGDM. Finally, Section 5 provides a numerical application of the methodologies for a new energy vehicle (NEV) research and development (R&D) task, with comparative and sensitivity analyses.

2. The framework of the proposed approach and preliminaries

This section details the approach's foundational concepts and presents the steps for implementing the decentralized multipartite consensus model within a hierarchical MAGDM system.

2.1. Problem description

Online review platforms are crucial for shaping consumer behavior and brand perception. However, the vast and varied UGC creates a complex, unstructured data environment. Traditional decision-making methods often overlook the subtleties of consumer opinions and struggle to integrate diverse perspectives, including expert views. This disconnect leaves a gap between the detailed information in reviews and the structured insights necessary for effective decision-making. The proposed framework addresses this issue by systematically organizing (UGC) into weighted decision attributes and implementing a collaborative decision-making mechanism. This mechanism integrates expert analysis, grounded in specialized domain knowledge and standardized assessment criteria, with collective user insights. The framework facilitates a balanced consensus through an iterative feedback loop, where expert and user assessments are integrated, refined, and carefully weighted. Consequently, decisions reflect both professional rigor and practical applicability.

Suppose there is a set of alternatives $X = \{x_1, \cdots, x_m, \cdots, x_M\}(M \geq 2)$ to be ranked which are evaluated based on an attribute system. The attribute system could have multiple layers. We consider a two-layer situation in this research. The upper layer attributes set is denoted as $A = \{A_1, \cdots, A_l, \cdots, A_L\}(L \geq 2)$ and the lower layer attributes set of A is denoted as $a = \{a_{1,1}, \cdots, a_{1,n_1}; \cdots; a_{l,1}, \cdots, a_{l,n_l}; \cdots; a_{L,1}, \cdots, a_{L,n_L}\}$, where $n_l(l = 1, \cdots, L)$ is the number of lower layer attributes corresponding to upper attribute A_l. The weights of L upper layer attributes are denoted by $W^A = \{W_l^A | l = 1, \cdots, L\}$, and $0 \leq W_l^A \leq 1\ (l = 1, \cdots, L)$, $\sum_{l=1}^{L} W_l^A = 1$. Similarly, the weights of lower layer attributes are $w^a = \left\{w_{1,1}^a, \cdots, w_{1,n_1}^a; \cdots; w_{l,1}^a, \cdots, w_{l,n_l}^a; \cdots; w_{L,1}^a, \cdots, w_{L,n_l}^a\right\}$, and $0 \leq w_{l,i} \leq 1\ (l = 1, \cdots, L, i = 1, \cdots, n_l)$, $\sum_{i=1}^{n_l} w_{l,i}^a = 1$. The set of evaluation grades to be used is $H = \{H_1, \cdots, H_n \cdots, H_N\}$. Besides, there are multi-party DMs from different stakeholder entities who are denoted as $SE = \{SE_1, \cdots, SE_p, \cdots, SE_P\}(P \geq 2)$, where P means the number of stakeholder entities. The set of DMs in the p_{th} stakeholder entity SE_p is denoted as $SE_p = \left\{dm_{p,1}, \cdots, dm_{p,k}, \cdots, dm_{p,n_p}\right\}$ where n_p signifies the number of DMs in SE_p. The relative weight of SE_p and $dm_{p,k}$ are signified by W_p^{SE} and $w_{p,k}^{dm}$ respectively, which satisfies $0 \leq W_p^{SE} \leq 1\ (p = 1, \cdots, P)$, $0 \leq w_{p,k}^{dm} \leq 1\ (k = 1, \cdots, n_p)$ and $\sum_{p=1}^{P} W_p^{SE} = 1$, $\sum_{k=1}^{n_p} w_{p,k}^{dm} = 1$.

2.2. Procedure of decentralized multipartite consensus model for MAGDM

The decentralized multipartite consensus model for MAGDM is shown in Fig. 1, which encompasses several critical stages: 1) Generation of the UXO attribute system based on UGC through text analysis and natural language processing (NLP), which identifies decision attributes that accurately reflect user perspectives. This process establishes a two-tier attribute framework. 2) The I-E responsive multi-granularity decision mechanism for MAGDM classifies stakeholder interests and expertise into four quadrants. The model dynamically adjusts attribute granularity according to DMs' expertise, employing fine-grained or coarse-grained distributed preference relations (DPR) for practical alternative evaluation. 3) A decentralized multipartite consensus mechanism introduces a robust system to manage consensus among diverse stakeholders. These stakeholders are categorized into distinct decision-making participative parties (DMPs) using the I-E matrix categorizes. The optimization models and feedback mechanisms are designed to align these varied perspectives to achieve consensus, ultimately leading to the selection of optimal alternatives.

2.3. Preliminaries

2.3.1. Preference relations

In this study, it is proposed that DMs perform their evaluations by conducting pairwise comparisons between pairs of alternatives. Expanding on LTS, the notion of a distributed linguistic preference relation (DLPR) was first presented (Zhang et al., 2014) to aid in the assessment of alternatives under conditions of uncertainty. Subsequently, a variety of frameworks for pairwise comparisons emerged to accommodate different evaluative scenarios, such as probabilistic linguistic preference relation (PLPR) (Zhang et al., 2016) and DPR (Fu et al., 2016).

Definition 1. (*Distributed preference relation (Fu et al., 2016)*) There exists an alternative set $X = \{x_1, \cdots, x_M\}$ that can be pairwisely compared by a series of evaluation grades $H = \{H_1, \cdots, H_N\}$ ($N > 2$ and N is an odd number). H_1 and H_N indicate inferior and superior levels, while $H_{(N+1)/2}$ signifies indifference. Specifically, $H_1, \cdots, H_{(N-1)/2}$ represent the grades with decreasing non-preferred intensity, while $H_{(N+3)/2}, \cdots, H_N$ denote the grades with increasing preferred intensity. The DPR matrix given by $dm_{p,k}$ is defined as $D_{p,k} \subset X \times X, D_{p,k} = (d_{ij}^{p,k})_{M \times M}$, where

$$d_{ij}^{p,k} = \left\{ \left(H_n, d_{ij}^{p,k}(H_n)\right), n = 1, \cdots, N; \left(H, d_{ij}^{p,k}(H)\right) \right\} \tag{1}$$

$d_{ij}^{p,k}(H_n)$ and $d_{ij}^{p,k}(H)$ denote the belief degree that alternative x_i is compared to x_j on grade H_n and ignorance by $dm_{p,k}$, respectively. $dm_{p,k}(H_n) \geq 0, d_{ij}^{p,k}(H) = d_{ji}^{p,k}(H) = 1 - \sum_{n=1}^{N} d_{ij}^{p,k}(H_n)$.

If $d_{ij}^{k}(H) = 0$, it is a complete assessment and vice versa. If $d_{ij}^{p,k}(H_n) > 0$, H_n is called a focal element. In the context of DPR in MAGDM, the ER approach conducts the fusion of different distributions in attributes/alternatives/experts levels (Yang and Xu, 2013; Zhou et al., 2022b). To relieve the burden of expressing assessment information, DMs are required to give comparisons between adjacent alternatives $d_{i,i+1}^{p,k}(i = 1, \cdots, M-1)$ rather than any pair of alternatives.

Suppose the evaluation grades in H are symmetrical, and the score value $s(H_n)$ of H_n satisfies $-1 = s(H_1) < \cdots < s(H_N) = 1$, $s\left(H_{(N+1)/2}\right) = 0$ and $s(H_n) = -s(H_{N-n+1})(n = 1, \cdots, N)$. Then DPR matrix

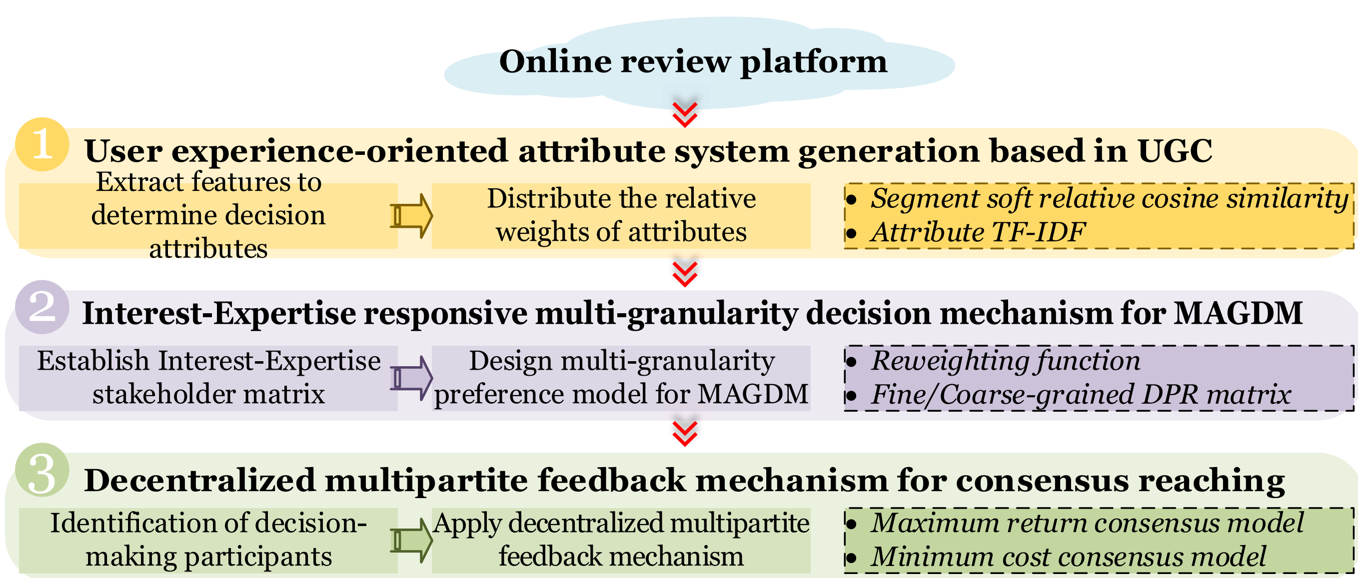

Fig. 1. The procedure of the decentralized multipartite consensus model for MAGDM.

$D^k = (d_{ij}^{p,k})_{M\times M}$ can be converted into a corresponding score matrix denoted by $S_{p,k} = \left(\left[S_{ij}^{(p,k)-}, S_{ij}^{(p,k)+}\right]\right)_{M\times M}$, where $S_{ij}^{(p,k)-} + S_{ji}^{(p,k)+} = 0$, $S_{ij}^{(p,k)+} + S_{ji}^{(p,k)-} = 0, \forall i,j \in \{1,\cdots,M\}$. After that, to infer the extent that x_i is preferred to x_j, the possibility degree (PD) matrix $PD_{p,k} = \left(pd_{ij}^{p,k}\right)_{M\times M}$ will be generated (Fu et al., 2019).

Definition 2. (*Dissimilarity measure between two DPRs* (Xue et al., 2021)) Let $D_{p,k} = \left(d_{ij}^{p,k}\right)_{M\times M}$ and $D_{p,g} = \left(d_{ij}^{p,g}\right)_{M\times M}$ be the DPRs provided by $dm_{p,k}$ and $dm_{p,g}$, respectively, where $p = 1,\cdots,P$; $k,g = 1,\cdots,n_p$; $k \neq g$. Then, the preference dissimilarity measure between $dm_{p,k}$ and $dm_{q,g}$ on the comparison of alternatives x_i and x_j can be calculated by

$$diss\left(d_{ij}^{p,k}, d_{ij}^{p,g}\right) = \frac{1}{2}\sum_{n=1}^{N-1}\sum_{n'=n+1}^{N} \psi_{ij}^{kg}(H_n)\psi_{ij}^{kg}(H_{n'})(s(H_{n'}) - s(H_n)) \tag{2}$$

where $\psi_{ij}^{kg}(H_n) = \left|d_{ij}^{p,k}(H_n) - d_{ij}^{p,g}(H_n)\right|$

2.3.2. Trust social network analysis

Within the scope of MAGDM, the involvement of DMs from various entities is particularly significant, as they often display intricate and dynamic social interactions rather than exist in isolation. Trust social network analysis (T-SNA) emerges as a specialized branch of SNA that concentrates on the complex network of trust relationships among DMs (Ji et al., 2023b).

Definition 3. (*Trust social network*) A trust social network can be represented by a directed graph $G(D,E)$ based on graph theoretic, in which the set of nodes $D = \{dm_1,\cdots,dm_k,\cdots,dm_{n_p}\}$ stands for individual DMs and directed lines set E indicates the trust relationship $\left(dm_k, dm_g\right)$ between DM pairs.

Definition 4.. (*Trust score matrix* (Wu et al., 2016)) DM dm_g evaluates his/her trust degree toward DM dm_k $(dm_g, dm_k \in SE_p, k \neq g)$ by trust function $\lambda_{gk} = (t_{gk}, d_{gk})$. $t_{gk}, d_{gk} \in [0,1]$ Indicate trust and distrust degrees from dm_g to dm_k with $t_{gk} + d_{gk} \in [0,1]$. Then, trust score for representing the trust relationship between the two DMs can be further obtained by:

$$ts_{gk} = \frac{t_{gk} - d_{gk} + 1}{2} \tag{3}$$

Obviously, $ts_{gk} \in [0, 1]$. On this basis, the trust score matrix $TS = \left[ts_{gk}\right]_{n_p\times n_p}$ can be obtained. Table 1 provides an example of the T-SNA among all DMs in SE_P.

Table 1
Trust social network analysis of SE_P

Trust social network	Trust score matrix
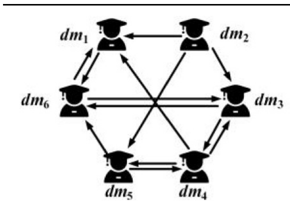	$TS = \begin{pmatrix} - & ts_{12} & - & ts_{14} & - & ts_{16} \\ ts_{21} & - & ts_{23} & - & ts_{25} & - \\ - & ts_{32} & - & ts_{34} & ts_{36} & \\ ts_{41} & - & ts_{43} & - & ts_{45} & \\ - & ts_{52} & - & ts_{54} & - & ts_{56} \\ ts_{61} & - & ts_{63} & ts_{64} & ts_{65} & - \end{pmatrix}$

3. User experience-oriented attribute system generation for MAGDM

In this section, a data-driven algorithm is first developed to generate the UXO attribute system and automatically determine attribute weights. The whole process is depicted in Fig. 2.

3.1. Extract features from UGC to determine decision attributes

This research enhances user experience analysis by thoroughly

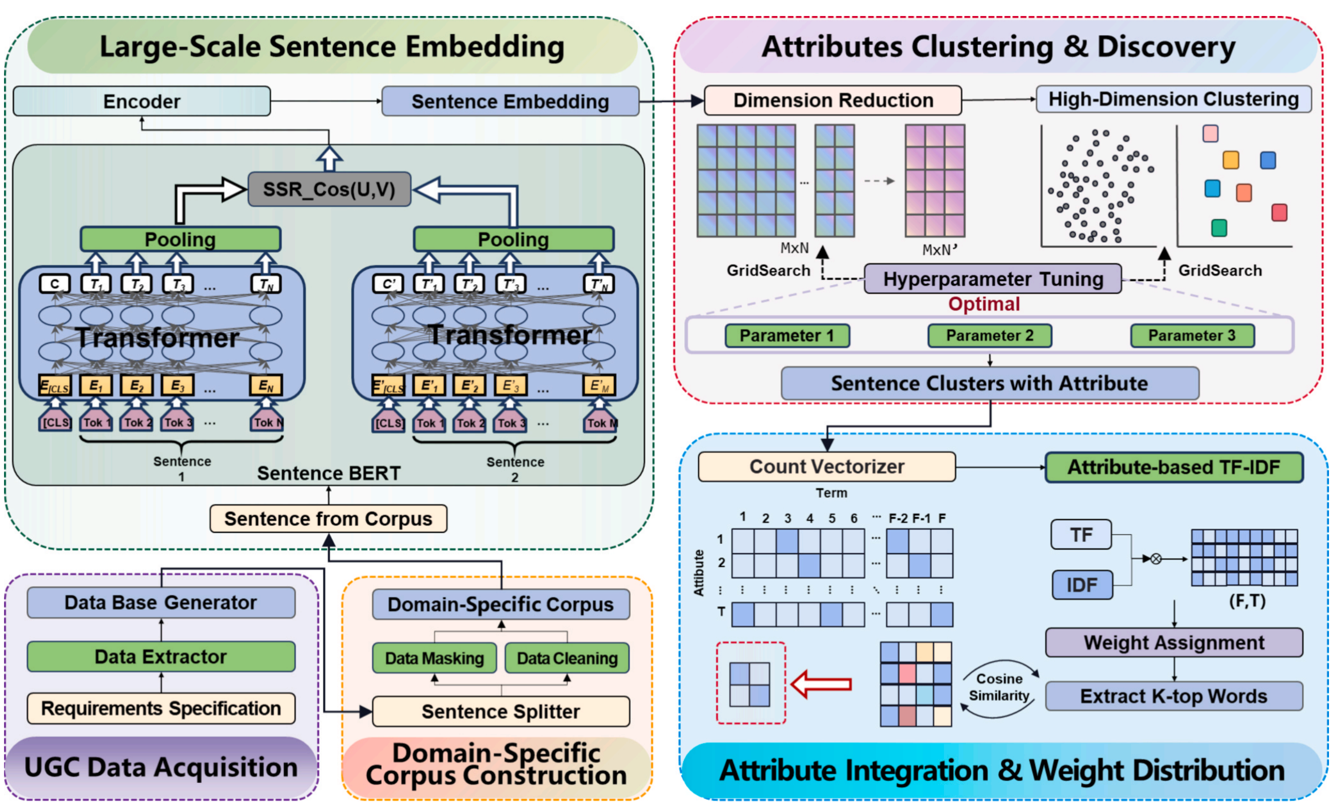

Fig. 2. The procedure of UXO attribute system generation based on UGC.

examining long texts and employing a vast corpus. Long texts reveal more about user sentiments and preferences because of their comprehensive content. Using a large corpus helps represent diverse user experiences effectively. However, this approach poses challenges, including advanced NLP tasks, the need for complex algorithms to understand context and semantics, and higher computational requirements. To overcome these obstacles, we developed a sophisticated text mining framework that efficiently processes and analyzes data from long texts and large corpora, ensuring accurate attribute determination in UGC.

Module 1. UGC data acquisition and domain-specific corpus construction

The methodology begins with corpus preparation, a vital step in data-driven decision-making. Data is collected using a database generator that employs algorithms to extract relevant UGC, enhanced by web crawling techniques to ensure comprehensive and relevant user experience data. Raw data is then transformed into a structured, domain-specific corpus. Advanced NLP techniques segment the data into sentences for contextual understanding. The data is anonymized, cleaned, and prepared for analysis, ensuring privacy compliance and relevance. We also define corpus quality measures to evaluate the effectiveness of this preparation process:

$$Q = \frac{N_{\text{relevant}}}{N_{\text{total}}} \times \frac{1}{N_{\text{errors}} + 1} \tag{4}$$

where N_{total} is the total number of sentences in the corpus, and N_{errors} is the number of errors or inconsistencies identified in the corpus. N_{relevant} represents the number of sentences that are identified as relevant. A sentence is considered relevant if it (i) contains domain-specific evaluative content, such as keywords or phrases indicating user sentiment and experience, and (ii) meets a minimum relevance score threshold determined by a combined lexical and statistical filtering process. Here, the relevance score is computed based on the occurrence of evaluative indicators and the semantic similarity with prototypical evaluative expressions in the domain. Eq. (4) reflects the dual objectives of maximizing relevance and minimizing errors in the corpus preparation process, thereby ensuring the quality and reliability of the data for subsequent analysis and decision-making.

Module 2. Large-scale sentence embedding

Large-scale sentence embedding aims to efficiently extract feature embeddings from domain-specific large corpora, addressing time constraints and dimensional curses. This module's innovation comprises: (i) Instead of the traditional matrix decomposition approach, which may blur distinctions in embeddings across large corpora (Landauer et al., 1998), we adopt a BERT-based model that delivers semantically rich and distinct sentence embeddings. (ii) While BERT excels in tasks like sentence classification and pair regression by generating fixed-size embeddings (e.g., averaging BERT's output (Zhao et al., 2022) or using the [CLS] token (Lan et al., 2019)), its cross-encoder structure is unsuitable for large-scale embedding due to the impractical number of inferences required. For instance, identifying the most similar pair in a collection of 10,000 sentences (M) requires nearly 50 million BERT inferences $\left(\frac{M\cdot(M-1)}{2} = 49{,}995{,}000\right)$, taking about 65 h on a modern V100 GPU.

Therefore, in this study, we leverage a sentence embedding technique based on a model analogous to SBERT (Reimers et al., 2019) and introduce a novel similarity metric, Soft Relative Cosine Similarity, to enhance the accuracy of embedding comparisons beyond what the original SBERT model achieves. SBERT modifies the traditional BERT architecture by incorporating Siamese and triplet network structures, enabling the direct comparison of generated sentence embeddings. However, these comparisons are typically limited to assessing cosine similarity at the directional level of the embeddings. To refine this approach, we first encode two sentences, S_1 and S_2, using the standard SBERT model, to obtain their respective embeddings, U and V. We then employ the *SSRcos* to evaluate the semantic correlation between these embeddings.

Definition 5. (*Segment soft relative cosine similarity between two sentence embeddings*) Let $U = [u_1, u_2, \cdots, u_T] \in \mathbb{R}^{1\times T}$ and $V = [v_1, v_2, \cdots, v_T] \in \mathbb{R}^{1\times T}$ be sentence embedding vectors partitioned into T' subvectors, where $D = T/T'$ represents the dimension of each subvector. Each subvector U_τ and V_τ for $\tau = 1, 2, \cdots, T'$ can be written as $U_\tau, V_\tau \in \mathbb{R}^{1\times D}$. Then, U and V can be represented as $U = [U_1, \cdots, U_\tau, \cdots, U_{T'}]$, $V = [V_1, \cdots, V_\tau, \cdots, V_{T'}]$. Therefore, the *SSRcos* can be calculated as follows:

$$SSR\cos(U,V) = \frac{\sum_{\tau=1}^{T'} \frac{\sum\sum_{i,j}^{D} s_{ij}^{\tau}\left(u_{\tau,i} - \overline{U}_\tau\right)\left(v_{\tau,j} - \overline{V}_\tau\right)}{\sqrt{\sum\sum_{i,j}^{D} s_{ij}^{\tau}\left(u_{\tau,i} - \overline{U}_\tau\right)\left(u_{\tau,j} - \overline{U}_\tau\right)}\sqrt{\sum\sum_{i,j}^{D} s_{ij}^{\tau}\left(v_{\tau,i} - \overline{V}_\tau\right)\left(v_{\tau,j} - \overline{V}_\tau\right)}}}{T'} \tag{5}$$

where $s_{ij}^{\tau} = sim(u_{\tau,i}, v_{\tau,j}) = \frac{1}{1+\sqrt{\left(u_{\tau,i}-v_{\tau,j}\right)^2}}$ captures the similarity between components of the segment vectors. And $\overline{U_\tau} = \sum_{i=1}^{D} u_{\tau,i}$, $\overline{V_\tau} = \sum_{i=1}^{D} v_{\tau,j}$.

Properties 1. (1) *Symmetry*: $SSRcos(U,V) = SSRcos(V,U)$.
(2) *Boundedness*: $SSRcos(U,V) \in [-1,1]$.
(3) *Positive definiteness*: For any non-zero U, $SSRcos(U,U) = 1$.
(4) *Identity of indiscernible*: $SSRcos(U,V)$ should be maximal iff U and V are equivalent after segmentation.

Remark 1. Eq. (5) introduces a mathematically intricate similarity measure well-suited for sentence embeddings. Fig. 3 compares traditional cosine similarity with the proposed *SSRcos*. Key features include: (1) Segmentation of embeddings: U and V are divided into T' subvectors, enabling local context evaluation and nuanced semantic detection. (2) Mean centering: Each segment $U\tau$ and $V\tau$ is mean-centered to minimize magnitude disparities and emphasize relative distribution. (3) Soft similarity measure: The similarity s_{ij}^{τ} between segment components use a soft function based on Euclidean distance, offering greater

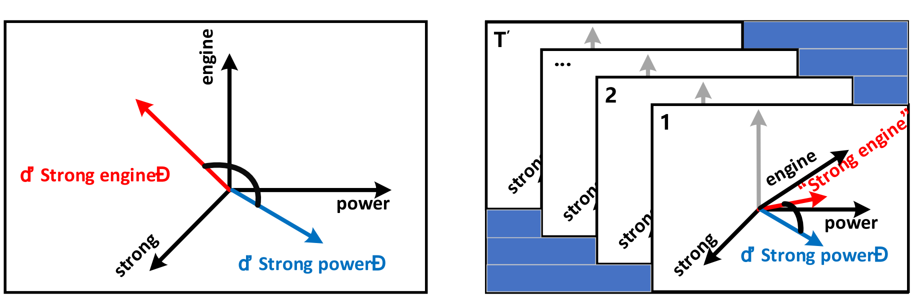

(a) (b)

Fig. 3. Comparison of vectors' representation (a) Cosine similarity (b) Segment soft relative cosine similarity between two sentence embeddings

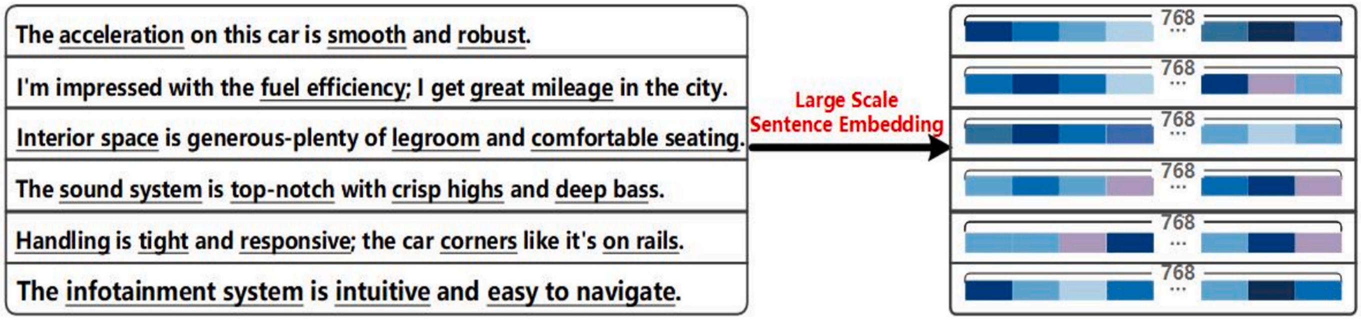

Fig. 4. Sentence embedding procedure

adaptability than traditional cosine similarity. (4) Aggregation across segments: The overall score is averaged from segment similarities, with equal segment contribution.

This similarity measure underpins various downstream tasks, including semantic search and clustering. By leveraging SBERT and *SSRcos*, we reduce the computational burden of pairwise comparisons, as embeddings are precomputed for efficient comparison, avoiding exhaustive BERT inferences. This approach saves time and mitigates the curse of dimensionality in large-scale corpora, making it highly effective for practical NLP applications. The PLM model is well-suited for large-scale corpora and semantic textual similarity (STS) tasks, embedding sentences into dense vectors to facilitate semantic similarity comparisons, as shown in Fig. 4.

Module 3. Attributes clustering and discovery

The attribute clustering and discovery module organizes high-dimensional sentence embeddings into distinct clusters for attribute discovery. Using enhanced SBERT in Module 2, we achieve a $[Num, 768]$ dimensional space, where '*Num*' represents the number of sentences in the corpus, and '768' the SBERT embedding dimensions. The complexity of UXO attribute tasks creates ambiguity in spatial locality, which can blur distances between points and affect clustering accuracy. To address this, we introduce a UMAP-assisted HDBSCAN clustering algorithm that reduces dimensionality while robustly clustering domain-specific corpora. UMAP compresses high-dimensional embeddings into a lower-dimensional space, preserving local and global structures by optimizing a weighted k-neighbor graph layout. HDBSCAN then clusters the reduced data, managing varied densities and noise without pre-defining cluster numbers. It calculates core distances to the σ^{th} nearest neighbor constructs a mutual reachability distance graph and forms a hierarchy of stable clusters condensed into flat clusters. These clusters are analyzed to identify key attributes and filter out noise. In experiments, tuning hyperparameters in the UMAP-assisted HDBSCAN is vital for optimized clustering. We use metrics like the Silhouette Coefficient (SC), Calinski-Harabasz (C-H) Score, and Davies-Bouldin (D-B) Index to refine hyperparameters iteratively, achieving clusters that are both meaningful and cohesive. Following this, an attribute integration module is developed that identifies and integrates the top K attributes most aligned with user preferences.

Module 4. Attribute integration and weight distribution

The module uses cosine similarity to refine coherent clusters of attributes. This module aims to consolidate these attributes into a representative set that captures UGC's core themes, emphasizing user preferences. The integration process begins with the Count Vectorizer, which converts text data into a feature vector, F, counting each term's frequency in the corpus. This process can be represented as: $F = \text{CountVectorizer}\ (\text{Corpus})$. Subsequently, an A-TF-IDF transformation is applied to the feature vector F to weigh the terms of F, which is defined in Definition 6.

Definition 6. (*Attribute-based TF-IDF*) Suppose there is a corpus C containing L attribute sets $\{A_1, \cdots, A_L\}$, which are composed of the terms $\{t_{1,1}, \cdots, t_{1,n_1}; \cdots; t_{L,1}, \cdots, t_{L,n_L}\}$. The domain corpus is processed to identify attributes clustered into sets. Each set of attributes A_l is considered a document as traditional TF-IDF. The A-TF-IDF is computed for each term of an attribute set. The TF of term $t_{l,i}$ in attribute set A_l is the number of times t_i appears in A_l, denoted as $f_{t_{l,i},A_l}$. The IDF of term $t_{l,i}$ is represented as $log\left[\frac{\sum_{l=1}^{L} n_l}{L\left(1+df_{t_{l,i}}\right)}\right]$, where $df_{t_{l,i}}$ is the number of attribute sets containing term $t_{l,i}$. The A-TF-IDF for term $t_{l,i}$ in A_l is then defined as:

$$TFIDF_{\text{Attribute}}\ \left(t_{l,i}, A_l\right) = f_{t_{l,i},A_l} \times log\left[\frac{\sum_{l=1}^{L} n_l}{L\left(1+df_{t_{l,i}}\right)}\right] \tag{6}$$

Unlike traditional weighting methods, this approach reduces the weight of terms frequently appearing across attribute sets while increasing the weight of rarer terms. Eq. (6) is applied to each term, generating a weighted score that emphasizes a term's significance within the specific domain. The strength of an attribute set is determined by summing its terms' TF-IDF scores. These aggregated scores calculate each set's overall relevance within the corpus. Correspondingly, the weight distribution for each term is determined starting with TF-IDF as the initial relative weight for the term of $t_{l,i}$, denoted as $W_{t_{l,i}}$. The K-top terms, representing the most preferred user features which defined as:

$$K\text{-top Terms } = \underset{t_{l,i}\in A_l}{argtop} - K\left(W_{t_{l,i}}\right) \tag{7}$$

In practice, K is determined such that the cumulative A-TF-IDF weight of the selected *top* $-k$ terms reach a predetermined threshold (e.g., 90 % of the total weight of attribute set A_l). This criterion ensures that the essential information within each attribute set is preserved without incorporating superfluous terms. Then, we remove irrelevant attributes by extracting only key weights to form a unified attribute set for the domain corpus. After that, the L attributes set $\{A_1, \cdots, A_L\}$ are updated into the same shape $(1, K)$, leading to the term's set $\{t_{1,1}, \cdots, t_{1,K}; \cdots; t_{L,1}, \cdots, t_{L,K}\}$. We refine our attribute aggregation process with these sets. Given the substantial, valuable data from large-scale corpora, directly applying dimensionality-reduced and clustered attribute sets as MAGDM indexes is suboptimal. Instead, we adopt an attribute integration method using an A-TF-IDF cosine similarity measure, defined below.

Definition 7. (*The similarity between attribute sets*) Let terms sets $\{t_{i,1}, \cdots, t_{i,K}\}$ and $\{t_{j,1}, \cdots, t_{j,K}\}$ belong to attribute sets A_i and A_j, respectively. The A-TF-IDF vectors for A_i and A_j are represented by V_i and V_j. The similarity between A_i and A_j can be calculated by

$$Similarity(A_i, A_j) = \frac{V_i \cdot V_j}{\|V_i\| \|V_j\|} \tag{8}$$

where $V_i \cdot V_j$ is the inner product of the TF-IDF vectors for attributes A_i and A_j, and $||V_i||$ and $||V_j||$ are the Euclidean norms of the TF-IDF vectors. This measurement quantifies the cosine of the angle between two vectors in the multidimensional space, reflecting how closely related the two attribute sets are in terms of their term compositions and significance within the corpus.

By using Definition 7, the similarity matrix $Similarity(A_i, A_j)_{L\times L}$ will be built, which is used to merge closely related attribute sets. The threshold is calculated by Eq. (9) by combining the mean similarity and standard deviation σ of $Similarity(A_i, A_j)_{L\times L}$.

$$\eta = \frac{1}{(L-1)(L-2)} \sum_{i=1}^{L-1} \sum_{j=i+1}^{L} \text{Similarity}(A_i, A_j) + 2\sigma \tag{9}$$

The final result of this module is a concise list of K-top attributes, which reflects the primary dimensions of user experience within the domain-specific corpus.

3.2. Determine the relative weights of attributes

After applying Modules 1–4, a UXO attribute system is established. Above all, we denote $A = \{A_1, \cdots, A_L\} (L \geq 2)$ as the attribute set which is the output of Module 4. The K-top terms $\{t_{1,1}, \cdots, t_{1,K}; \cdots; t_{L,1}, \cdots, t_{L,K}\}$ of A is denoted as $a = \{a_{1,1}, \cdots, a_{1,n_1}; \cdots; a_{L,1}, \cdots, a_{L,n_L}\}$, which generated by removing duplicate. a is lower layer attributes set of A, where $n_l (l = 1, \cdots, L)$ is the actual number of lower layer attributes of their upper-level attribute set A_l. The weights of L upper- and lower-layer attribute sets are calculated by **Definitions 8 and 9.**

Definition 8. (*Attribute set weight distribution*) The weight of attribute set A_l is represented by W_l^A, which is calculated by the sum of the A-TF-IDF scores for all terms in A_l as Eq. (10).

$$W_l^A = \sum_i^{n_l} \text{TF-IDF}_{\text{attribute}}(t_{l,i}, A_l) \tag{10}$$

Definition 9. (*Normalization of attribute weights*) Suppose $a = \{a_{1,1}, \cdots, a_{1,n_1}; \cdots; a_{L,1}, \cdots, a_{L,n_L}\}$ is lower layer attributes in an attribute set $A = \{A_1, \cdots, A_l, \cdots, A_L\}$. The relative weight of $a_{l,i}$ ($a_{l,i} \in A_l$) is calculated as:

$$w_{l,i}^a = \frac{\text{TF-IDF}_{\text{Attribute}}(a_{l,i}, A_l) - \min\limits_{i=1,\cdots,n_l} \text{TF-IDF}_{\text{Attribute}}(a_{l,i}, A_l)}{\max\limits_{i=1,\cdots,n_l} \text{TF-IDF}_{\text{Attribute}}(a_{l,i}, A_l) - \min\limits_{i=1,\cdots,n_l} \text{TF-IDF}_{\text{Attribute}}(a_{l,i}, A_l)} \tag{11}$$

The whole UXO attribute system generation algorithm procedure is shown in Algorithm 1.

Algorithm 1 (UXO attribute system generation)

```
Input: A domain of interest for UGC data acquisition
Output: UXO attribute system
Module 1: UGC Data Acquisition and Domain-Specific
  Corpus Construction
function OPTIMIZE_CORPUS_CONSTRUCTION(domain):
  best_Q ← −∞
  best_corpus ← None
  database_generator ← INITIALIZE_DATABASE_GENERATOR()
  for n ← 1 to MaxIterationNum while
   best_Q < MaxQualityNum do
     raw_data ←
       ACQUIRE_DATA(database_generator, domain)
     corpus ← PROCESS_CORPUS(raw_data)
     Q ← CALCULATE_CORPUS_QUALITY(corpus)
     if Q > best_Q then
        best_Q ← Q
        best_corpus ← corpus
     end
  end
  return best_corpus
Module 2: Large-Scale Sentence Embedding
function EMBEDDED_SENTENCES(corpus):
  model ← InitializeModel()
  embeddings ← []
  for i ← 1 to |corpus| do
     model ←
       LOAD_SBERT_MODEL_WITH_CUSTOM_LOSS(u, v)
     embedding ← model.verify(corpus[i])
     embeddings.append(embedding)
  end
  return embeddings
Module 3: Attributes Clustering and Discovery
function
 CLUSTER_AND_OPTIMIZE_ATTRIBUTES(embeddings):
  reduced_embeddings ← []
   metrics_set ← [SC, D−B, C−H] initialize
   hyperparameter set ℬ and cluster set C
  foreach e in embeddings do
     r ← REDUCE_DIMENSIONS(e)
     reduced_embeddings.append(r)
  end
  foreach metric in metrics_set do
     foreach b ∈ ℬ do
        compute score s under metric
        clusters ←
          COUNT_CLUSTERS(reduced_embeddings, b)
        if s increased then
           update best clusters for metric
        end
     end
     C.append(clusters)
  end
  visualize C
  (optimal_clusters, optimal_params) ←
   FIND_OPTIMAL_CLUSTERS(C)
  return optimal_clusters
Module 4: Attribute Integration and Weight Distribution
function AGGREGATE_AND_RANK_ATTRIBUTES(clusters):
  initialize iteration count and convergence threshold
  feature_vectors ←
   CONVERT_TO_FEATURE_VECTORS(clusters)
  initialize similarity matrix and attribute_weights
  repeat
     attribute_weights ←
       CALCULATE_ATTRIBUTE_TF-IDF(feature_vectors)
     update similarity matrix using attribute_weights
     if matrix converges then
        K_top_attributes ←
          SELECT_K_TOP_ATTRIBUTES(attribute_weights)
        refine feature_vectors using K_top_attributes
     end
     increment iteration count
  until convergence or max iterations reached
  return K_top_attributes
```

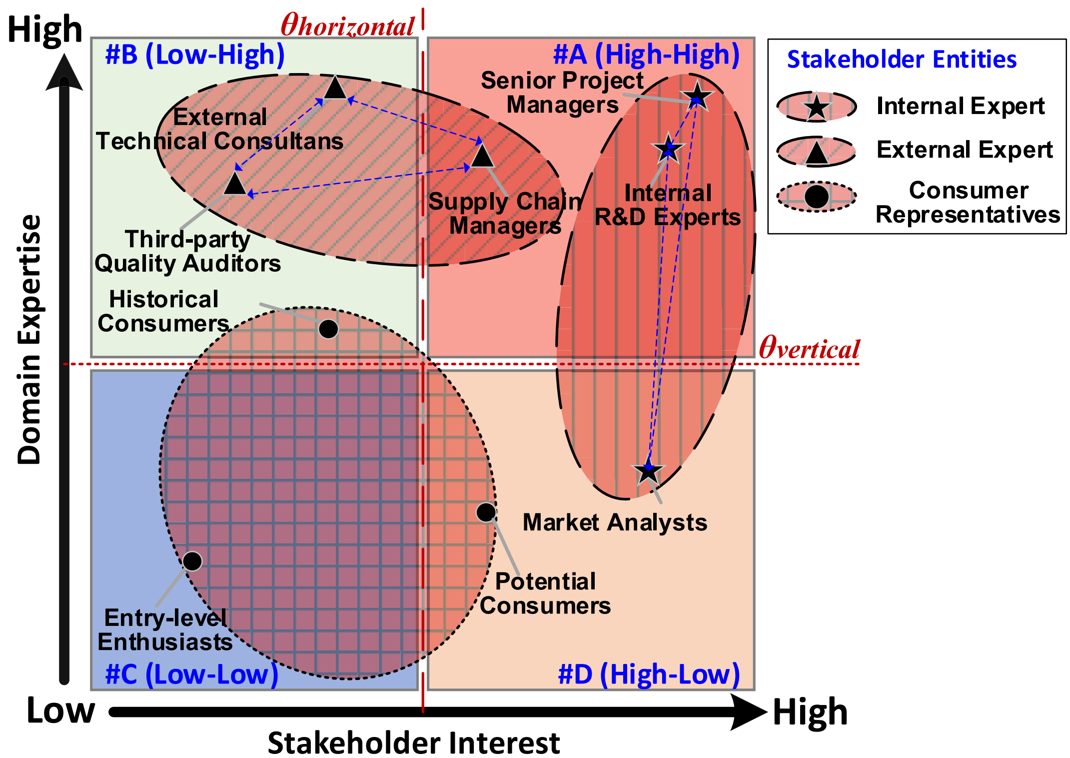

Fig. 5. I-E analysis model.

4. Decentralized multipartite consensus mechanism for MAGDM

This section presents a decentralized multipartite consensus mechanism for MAGDM, utilizing the earlier established I-E responsive framework. It integrates a two-layered attribute system to assist DMs of different expertise levels in engaging effectively. Additionally, it introduces a multipartite feedback mechanism that incorporates various stakeholder views.

4.1. I-E responsive multi-granularity decision mechanism for MAGDM

In Section 3.1, we developed a UXO attribute system with a two-layer framework. The upper layer includes coarse-grained attributes such as performance, comfort, and design, covering general aspects of user experience. The lower layer offers detailed, fine-grained attributes like acceleration smoothness, seat ergonomics, and aesthetic details. This approach accommodates the varied preferences of DMs with different professional backgrounds and knowledge levels when evaluating alternatives.

4.1.1. Establish Interest-Expertise stakeholder matrix

On this basis, a novel I-E matrix is proposed that draws inspiration from Mendelow's Power-Interest matrix. This matrix is characterized by two axes: the X-axis represents stakeholder interest, and the Y-axis depicts DM's domain expertise. It is segmented into four distinct quadrants by two thresholds ($\theta_{horizontal}/\theta_{vertical}$), as shown in Fig. 5. Here, **#A. (IE^{H-H})** involves the core team members, including senior project managers, supply chain managers and internal R&D experts, whose in-depth knowledge and high interest drive the project's development. **#B. (IE^{L-H})** is typically composed of external experts or consumers, such as third-party quality auditors or technical consultants. They possess profound domain knowledge but might have an irrelevant interest regarding the project's result. **#C. (IE^{L-L})** includes stakeholders like entry-level enthusiasts, who have limited influence on technical decisions and lack deep knowledge of the project domain. **#D. (IE^{H-L})** includes stakeholders such as potential consumers and market analysts who show strong interest in product R&D despite lacking technical expertise. Visible features and overall market presence influence their perceptions.

Remark 2. Recognizing that a single entity might cross multiple quadrants due to the diversity of interests and expertise levels is important. As shown in Fig. 5, different consumer types are in quadrants #B, #C and #D. These range from highly interested but technically inexperienced individuals focused on product benefits (#D), to those with some technical knowledge but less direct impact from outcomes (#B), and passive consumers with limited domain knowledge (#C). This diversity highlights the need for a decision-making approach tailored to different expertise and interest levels. Internal experts typically occupy quadrants #A and #D, such as project managers and R&D specialists, who possess high expertise and interest (#A). External DMs span quadrants #A and #B, including technical consultants, quality auditors with high expertise but less vested interest (#B), and supply chain managers who combine specialized knowledge with a substantial stake in project success (#A).

To more comprehensively measure the X-axis, Y-axis, and demarcation threshold in the I-E matrix, we employ a combination of quantitative and qualitative assessment as defined in Definitions 10 and 11.

Definition 10. (*Stakeholder interest level measurement*) The interest of $dm_{p,k}$ can be assessed through a multi-criteria measurement incorporating both qualitative and quantitative elements. The function $SIL(dm_{p,k})$ representing the stakeholder interest level (SIL) of DM $dm_{p,k}$ is defined as:

$$SIL(dm_{p,k}) = \gamma_1 \cdot ROI(dm_{p,k}) + \gamma_2 \cdot SEL(dm_{p,k}) + \gamma_3 \cdot IVS(dm_{p,k}) \tag{12}$$

The return on involvement (ROI) of $dm_{p,k}$ is calculated by $ROI(dm_{p,k}) = \frac{(\mathrm{BOI}(dm_{p,k}) - \mathrm{COI}(dm_{p,k}))}{\mathrm{COI}(dm_{p,k})} \in [0,1]$, where $\mathrm{BOI}(dm_{p,k})/\mathrm{COI}(dm_{p,k})$ signify the benefit/cost of $dm_{p,k}$'s involvement. ROI measures the perceived value stakeholders gain from their involvement relative to the effort they have made. The stakeholder engagement level (SEL) of $dm_{p,k}$ is obtained by $SEL(dm_{p,k}) = \frac{FOE(dm_{p,k}) \times IOE(dm_{p,k})}{TPEO(dm_{p,k})} \in [0,1]$, which captures the frequency and depth of stakeholder interactions in project-related activities. $FOE(dm_{p,k})/IOE(dm_{p,k})/TPEO(dm_{p,k})$ denote the frequency of engagement/intensity of engagement/total possible engagement opportunities of $dm_{p,k}$. Interest valuation score $IVS(dm_{p,k}) \in [0,1]$ reflects the self-assessed value derived from the project by $dm_{p,k}$. $\gamma_1, \gamma_2, \gamma_3$ are weighting coefficients summing to 1, adjusted to reflect the relative importance of each metric. Then the threshold $\theta_{horizontal}$ can be set as:

$$\theta_{horizontal} = \mu_{SIL} + \gamma' \sigma_{SIL} \tag{13}$$

where $\mu_{SIL} = \frac{\sum_{p=1}^{P}\sum_{k=1}^{n_p} SIL(dm_{p,k})}{\sum_{p=1}^{P} n_p}$, $\sigma_{SIL} = \sqrt{\frac{\sum_{p=1}^{P}\sum_{k=1}^{n_p}\left(SIL(dm_{p,k}) - \mu_{SIL}\right)^2}{\sum_{p=1}^{P} n_p}}$, γ' is an adjustment coefficient. A higher value of γ' stands for a stricter standard of high interest, thereby narrowing the high-interest group to the most engaged stakeholders. This adjustment allows for the application of the model to specific organizational contexts and stakeholder dynamics.

Remark 3. ($ROI(dm_k)$) is the variation of return on investment, focusing on engagement aspect. Benefits include knowledge acquisition, network expansion or direct financial gains, while costs could be time or resources. Besides, $SEL(dm_k)$ measures each instance of engagement (e.g., meetings, feedback sessions) weighted by the depth of involvement (e.g., active participation vs. passive attendance). $IVS(dm_k)$ is a subjective value of DM.

Example 1.. Suppose there are 3 DMs coming from different stakeholder entities SE_1, SE_2 and SE_3, which denote internal experts, external experts and consumer representatives, respectively. Suppose the weighting coefficients are equally distributed: $\gamma_1 = \gamma_2 = \gamma_3 = \frac{1}{3}$. $SIL(dm_{1,1}) = \frac{1}{3} \times \frac{80-60}{60} + \frac{1}{3} \times \frac{15\times 0.8}{20} + \frac{1}{3} \times 0.8 = 0.591$, $SIL(dm_{2,1}) = \frac{1}{3} \times \frac{35-30}{30} + \frac{1}{3} \times \frac{10\times 0.6}{15} + \frac{1}{3} \times 0.5 = 0.444$, $SIL(dm_{3,1}) = \frac{1}{3} \times \frac{12-10}{10} + \frac{1}{3} \times \frac{1\times 0.4}{1} + \frac{1}{3} \times 0.2 = 0.267$. When $\gamma' = 1$, $\theta_{horizontal} = 0.434 + 0.132 = 0.566$. The detailed numerical case and explanation can be found in Supplementary Materials' Part A.

Definition 11. (*Domain expertise level measurement*) DM's domain expertise is measured through an integration of peer evaluation and knowledge testing. Function $DEL(dm_{p,k})$ representing the domain expertise level (DEL) of DM $dm_{p,k}$ is defined as:

$$DEL(dm_{p,k}) = \delta_1 \cdot PTS(dm_{p,k}) + \delta_2 \cdot \mathrm{KDI}(dm_{p,k}) \tag{14}$$

Here, the peer-reviewed trust score (PTS) of $dm_{p,k}$ is calculated by $PTS(dm_{p,k}) = \frac{1}{n_p - 1}\sum_{g \neq k} ts_{gk}(dm_{p,k}, dm_{p,g} \in SE_p)$ where ts_{gk} stands for the trust score from $dm_{p,g}$ towards $dm_{p,k}$ which is calculated by Eq. (3). KDI $(dm_{p,k}) \in [0,1]$ is the knowledge dissemination index of $dm_{p,k}$ based on contributions to domain knowledge pools and active communication within the R&D community. δ_1 and δ_2 are the respective weights of trust and contribution measures, $\delta_1 + \delta_2 = 1$. The threshold $\theta_{vertical}$ can be established as:

$$\theta_{\mathrm{vertical}} = \mu_{DEL} + \delta' \sigma_{DEL} \tag{15}$$

where $\mu_{DEL} = \frac{\sum_{p=1}^{P}\sum_{k=1}^{n_p} DEL(dm_{p,k})}{\sum_{p=1}^{P} n_p}$, $\sigma_{DEL} = \sqrt{\frac{\sum_{p=1}^{P}\sum_{k=1}^{n_p}\left(DEL(dm_{p,k}) - \mu_{DEL}\right)^2}{\sum_{p=1}^{P} n_p}}$, δ' is an adjustment coefficient.

By using **Definitions 10 and 11**, each $dm_{p,k}$ can be identified into different I-E region by the $[SIL(dm_{p,k}), DEL(dm_{p,k})]$ and the value of $\theta_{horizontal}, \theta_{vertical}$. The discriminant formulas are given as follows:

$$\begin{cases} IE^{(H-H)} = \{dm_{p,k} | SIL(dm_{p,k}) \geq \theta_{horizontal} \wedge DEL(dm_{p,k}) \geq \theta_{vertical}\} \\ IE^{(L-H)} = \{dm_{p,k} | SIL(dm_{p,k}) < \theta_{horizontal} \wedge DEL(dm_{p,k}) \geq \theta_{vertical}\} \\ IE^{(L-L)} = \{dm_{p,k} | SIL(dm_{p,k}) < \theta_{horizontal} \wedge DEL(dm_{p,k}) < \theta_{vertical}\} \\ IE^{(H-L)} = \{dm_{p,k} | SIL(dm_{p,k}) \geq \theta_{horizontal} \wedge DEL(dm_{p,k}) < \theta_{vertical}\} \end{cases} \tag{16}$$

Example 2. Continue with **Example 1**, let's assume the weighting coefficients for the domain expertise level formula are equally distributed: $\delta_1 = \delta_2 = \frac{1}{2}$. $DEL(dm_{1,1}) = 0.75$, $DEL(dm_{2,1}) = 0.87$, $DEL(dm_{3,1}) = 0.275$. When $\delta' = 1$, $\theta_{\mathrm{vertical}} = 0.867$. Therefore, $dm_{1,1} \in \boldsymbol{IE}^{L-L}$, $dm_{2,1} \in \boldsymbol{IE}^{L-H}$, $dm_{3,1} \in \boldsymbol{IE}^{L-L}$. The detailed numerical case and explanation can be found in Supplementary Materials' Part A.

4.1.2. Multi-granularity preference model for MAGDM

Given the diverse expertise levels in the I-E matrix, aligning the decision-making process with attribute granularity is crucial. High-expertise DMs benefit from fine-grained attributes, enabling more profound insights and informed decisions. Conversely, less expert DMs may prefer coarse-grained attributes that offer a broader overview and simplify decision-making. The MAGDM framework adapts flexibly to these differences, effectively addressing uncertainty. DM $dm_{p,k}$ should evaluate alternatives by using either the fine-grained DPR matrix ($DEL(dm_{p,k}) \geq \theta_{vertical}$) or the coarse-grained DPR matrix ($DEL(dm_{p,k}) < \theta_{vertical}$) based on $DEL(dm_{p,k})$.

Definition 12. (*Fine-grained DPR matrix*) If $DEL(dm_{p,k}) \geq \theta_{vertical}$ $(dm_{p,k} \in \{IE^{(H-H)} \vee IE^{(L-H)}\})$, DM $dm_{p,k}(p = 1, \cdots, P; k = 1, \cdots, n_p)$ will evaluate M alternatives $X = \{x_1, \cdots, x_m, \cdots, x_M\}$ on a two-layer attribute system. The weight is $w^a = \{w^a_{1,1}, \cdots, w^a_{1,n_1}; \cdots; w^a_{L,1}, \cdots, w^a_{L,n_l}\}$. The fine-grained frame of discernment to be used by $dm_{p,k}$ is $H^{p,k} = \{(H_1)^{p,k}, \cdots, (H_n)^{p,k}, \cdots, (H_N)^{p,k}\}$ (N is an odd number). The fine-grained DPR is given by $dm_{p,k}$ for comparing alternatives x_i and x_j on attribute $\{a_{l,1}, \cdots, a_{l,n_l}\} \in A_l (l = 1, \cdots, L)$ is:

$$d^{p,k}_{l,(ij)} = \left\{\left((H_n)^{p,k}, f^{p,k}_{l,(ij)}\left[(H_n)^{p,k}\right]\right), n = 1, \cdots, N; \left(H^{p,k}, f^{p,k}_{l,(ij)}(H^{p,k})\right)\right\} \quad (l = 1, \cdots, L) \tag{17}$$

where $f^{p,k}_{l,(ij)}\left[(H_n)^{p,k}\right]$ and $f^{p,k}_{l,(ij)}(H^{p,k})$ stand for the belief degree on $(H_n)^{p,k}$ and global ignorance, $f^{p,k}_{l,(ij)}\left[(H_n)^{p,k}\right] = \frac{\sum_{v=1}^{n_l}\widetilde{w}^{p,k}_{l,v} \cdot \left|H^{p,k}_{n,l,ij}(a_{l,v})\right|}{\sum_{v=1}^{n_l}\widetilde{w}^{p,k}_{l,v}}$ and $f^{(p,k)}_{l,(ij)}(H) = \frac{\sum_{v=1}^{n_l}\widetilde{w}^{p,k}_{l,v} \cdot \left|H^{p,k}_{l,(ij)}(a_{l,v})\right|}{\sum_{v=1}^{n_l}\widetilde{w}^{p,k}_{l,v}}$. $\left|H^{p,k}_{n,l,(ij)}(a_{l,v})\right|$ and $\left|H^{p,k}_{l,(ij)}(a_{l,v})\right|$ represent the number of attributes $a_{l,v}$ that $dm_{p,k}$ evaluates for x_{ij} on $(H_n)^{p,k}$ and $H^{p,k}$. $\widetilde{w}^{p,k}_{l,v} = \frac{w^a_{l,v}}{1 + w^a_{l,v} - r^{p,k}_{l,v}}$ represents an adjusted weight of $a_{l,v}$ by combining the original weight $w^a_{l,v}$ and the relative importance $r^{p,k}_{l,v}$ given by $dm_{p,k}$. Specifically, when the relative importance equals to the original weight $\left(r^{p,k}_{l,v} = w^a_{l,v}\right)$, the adjusted weight remains unchanged $\left(\widetilde{w}^{p,k}_{l,v} = w^a_{l,v}\right)$. It is easy to note that $\sum_{n=1}^{N} f^{p,k}_{l,(ij)}\left[(H_n)^{p,k}\right] + f^{p,k}_{l,ij}(H^{p,k}) = 1$.

Definition 13. (*Coarse-grained DPR matrix*) If $DEL(dm_{p,k}) < \theta_{vertical}$ $(dm_{p,k} \in \{IE^{(H-L)} \vee IE^{(L-L)}\})$, DM $dm_{p,k}(p = 1, \cdots, P; k = 1, \cdots, n_p)$ will only evaluate M alternatives $X = \{x_1, \cdots, x_m, \cdots, x_M\}$ on the upper attribute set $A = \{A_1, \cdots, A_l, \cdots, A_L\}$. The coarse-grained frame of discernment by $dm_{p,k}$ is $H^C = \{H^C_1, \cdots, H^C_n, \cdots, H^C_N\}$ (N is an odd number). The coarse-grained DPR given by $dm_{p,k}$ for comparing alternative x_i and x_j

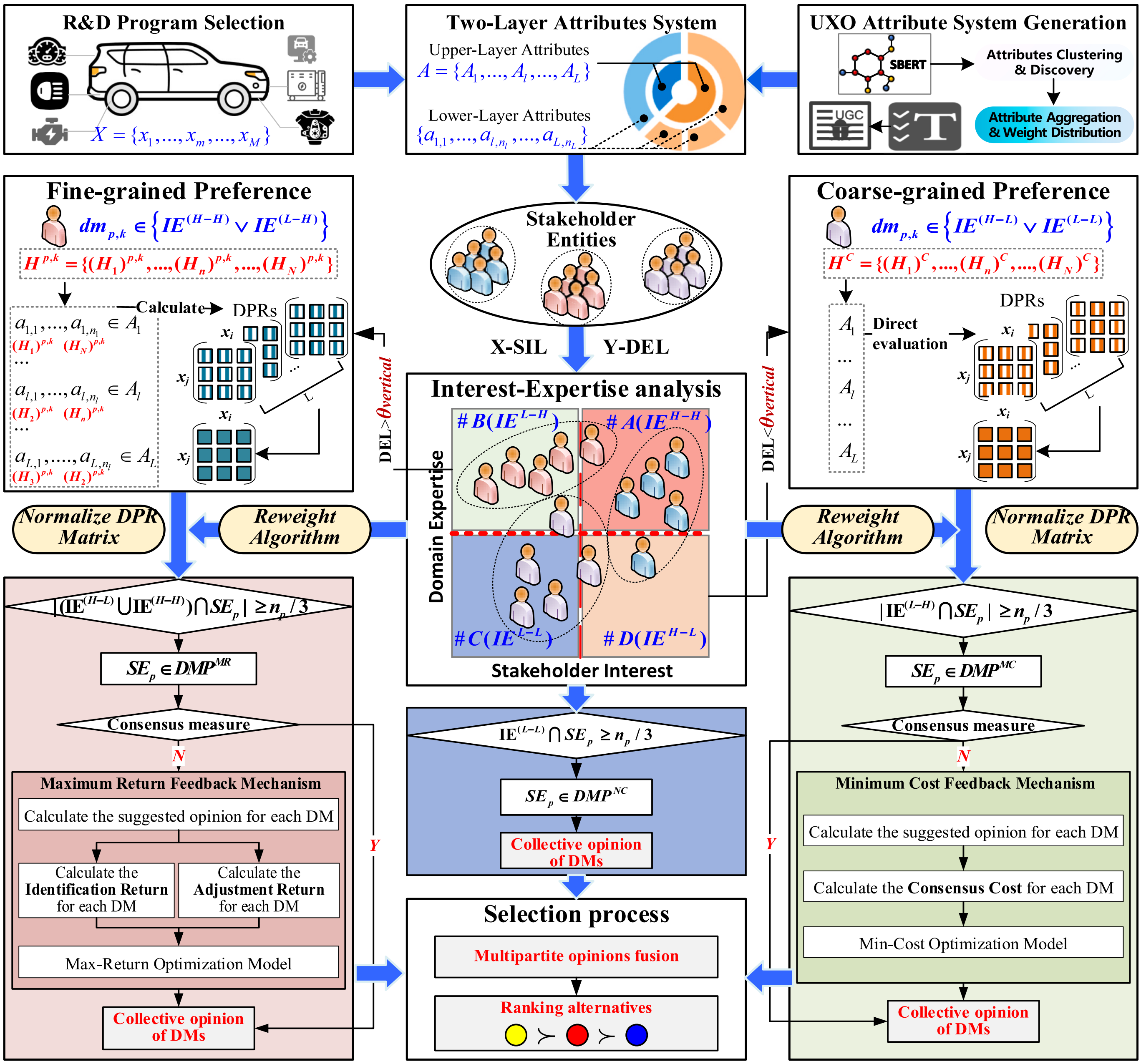

Fig. 6. Decentralized multipartite consensus mechanism for MAGDM.

on A_l is defined as:

$$d^{p,k}_{l,(ij)} = \left\{ \left(H^C_n, c^{p,k}_{l,(ij)}\left(H^C_n\right)\right), n = 1, \cdots, N; \left(H^C, c^{p,k}_{l,(ij)}\left(H^C\right)\right) \right\} \quad (l = 1, \cdots, L) \tag{18}$$

Similarly, $c^{p,k}_{l,(ij)}\left(H^C_n\right)$ and $c^{p,k}_{l,(ij)}\left(H^C\right)$ stand for the belief degree on H^C_n and global ignorance, and $\sum_{n=1}^{N} c^{p,k}_{l,(ij)}\left(H^C_n\right) + c^{(p,k)}_{l,(ij)}\left(H^C\right) = 1$.

Remark 4. There are two types of ignorance $f^{p,k}_{l,(ij)}\left(H^{p,k}\right)$ and $c^{p,k}_{l,(ij)}\left(H^C\right)$ caused by different granularity of evaluation. The former is a statistically inferred value reflecting a DM's ignorance of specific fine-grained attributes. DM directly provides the latter due to the global ignorance of a coarse-grained attribute. Although similar in form, they differ in meaning and computation methods.

After obtaining the DPRs for different regions of DMs within the multi-granularity frame of discernment, a crucial step is to ascertain the weights of attributes and DMs, especially when faced with significant uncertainty. This study addresses two forms of uncertainty: aleatoric uncertainty (AU), which reflects the inherent randomness in system outcomes or properties, and epistemic uncertainty (EU), arising from incomplete domain knowledge. We employ Shannon entropy as a measure of belief entropy to evaluate the reliability of the evidence provided by DMs. Shannon entropy measures the spread or dispersion of belief degrees, providing insights into the uncertainty or precision of the DMs' judgments. High entropy values indicate a more dispersed belief system, suggesting higher uncertainty, while lower values denote more concentrated beliefs, indicating more decisive preferences.

Definition 14. (*Belief entropy of fine-grained DPRs*) Suppose fine-grained DPRs by DMs as $d^{p,k}_{l,(ij)} = \left\{\left((H_n)^{p,k}, f^{p,k}_{l,(ij)}\left[(H_n)^{p,k}\right]\right), n = 1, \cdots,\right.$

$N;\left(H^{p,k}, f^{p,k}_{l,(ij)}\left(H^{p,k}\right)\right)\}$. The belief entropy is calculated as:

$$E\left(d^{p,k}_{l,(ij)}\right) = -BD^{p,k}_{l,(ij)}\log_2 BD^{p,k}_{l,(ij)} \tag{19}$$

where $BD^{p,k}_{l,(ij)} = 1 - \frac{\left|H^{p,k}_{l,(ij)}(a_{l,v})\right|}{n_l}$ signifies the sum of belief degrees to all the N grades on x_{ij} in evaluating A_l by $dm_{p,k}$. And $\left|H^{p,k}_{n,l,(ij)}(a_{l,v})\right|$ represents the number of attributes $a_{l,v}$ that $dm_{p,k}$ evaluates for x_{ij} on $(H_n)^{p,k}$.

Definition 15. (*Belief entropy of coarse-grained DPRs*) The coarse-grained DPR given by $dm_{p,k}$ for comparing alternative x_i over x_j on A_l is represented as $d^{p,k}_{l,(ij)} = \left\{\left(H^C_n, c^{p,k}_{l,(ij)}\left(H^C_n\right)\right), n = 1, \cdots, N; \left(H^C, c^{p,k}_{l,(ij)}\left(H^C\right)\right)\right\}$. The bodies of evidence (BOE) is denoted by $\mathfrak{B}^C_{l,(ij)} = \left\{H^C_n \middle| c^{p,k}_{l,(ij)}\left(H^C_n\right) > 0, H^C_n \subseteq H^C\right\}$. Then, the belief entropy of $d^{p,k}_{l,(ij)}$ is computed as:

$$E\left(d^{p,k}_{l,(ij)}\right) = -\sum\nolimits_{H^C_n \subseteq \mathfrak{B}^C_{l,(ij)}} c^{p,k}_{l,(ij)}\left(H^C_n\right)\log_2 c^{p,k}_{l,(ij)}\left(H^C_n\right) \tag{20}$$

Therefore, based on Eqs. (19)-(20), the average belief entropy on attributes, alternatives, and DMs are calculated by Eqs. (21)-(23) as:

$$E\left(d^{p,k}_{l}\right) = \frac{\sum_{1<i<M-1, j=i+1} E\left(d^{p,k}_{l,(ij)}\right)}{M-1} \tag{21}$$

$$E\left(d^{p,k}_{(ij)}\right) = \frac{\sum_{l=1}^{L} E\left(d^{p,k}_{l,(ij)}\right)}{L} \tag{22}$$

$$E\left(dm_{p,k}\right) = \frac{\sum_{1<i<M-1, j=i+1} E\left(d^{p,k}_{(ij)}\right)}{M-1} \tag{23}$$

As for the upper layers $A = \{A_1, \cdots, A_L\}$, the initial weights W^A_l are generated by Algorithm 2. By further taking consideration of AU and EU, the adjusted weights $\widetilde{W}^{p,k}_l$ are calculated as:

$$\widetilde{W}^{p,k}_l = \frac{W^A_l}{1 + W^A_l - R^{p,k}_l} \tag{24}$$

where $R^{p,k}_l = \frac{1-\widetilde{E}\left(d^{p,k}_l\right)}{L-\sum_{l=1}^{L}\widetilde{E}\left(d^{p,k}_l\right)}$ and $\widetilde{E}\left(d^{p,k}_l\right) = \frac{E\left(d^{p,k}_l\right)}{\sum_{l=1}^{L} E\left(d^{p,k}_l\right)}$ signifies the reliability of $dm_{p,k}$ for evaluating all alternatives on A_l and the normalized belief entropy of Eq. (21). This formula uses entropy to measure the unpredictability or dispersion of DMs' belief degrees across alternatives. Higher entropy indicates greater uncertainty or lower confidence, often due to variability in the decision-making environment or knowledge gaps. By subtracting normalized entropy from 1, the formula inversely relates greater uncertainty to lower reliability.

When considering the AU and EU generated by $dm_{p,k}$, the former can be calculated by belief entropy. The latter may be derived from differences in the selection and identification framework of experts at different professional levels and the uncertainty of the evaluation itself given by DMs. The reweighted relative weight of $dm_{p,k}$ is calculated as follows:

$$\widetilde{w}^{dm}_{p,k} = \frac{w^{dm}_{p,k}}{1 + w^{dm}_{p,k} - r^{dm}_{p,k}} \tag{25}$$

where $w^{dm}_{p,k} = \frac{\exp\left(DEL\left(dm_{p,k}\right)\right)}{\sum_{k=1}^{n_p}\exp\left(DEL\left(dm_{p,k}\right)\right)}$, $r^{dm}_{p,k} = \frac{1-\widetilde{E}\left(dm_{p,k}\right)}{n_p-\sum_{k=1}^{n_p}\widetilde{E}\left(dm_{p,k}\right)}$. $w^{dm}_{p,k}$ signifies the original relative weight of $dm_{p,k}$ caused by the difference in DEL, which reflects the EU of DM. The reliability $r^{dm}_{p,k}$ is established for measuring the AU of $dm_{p,k}$. Similarly, the reweighted weight of SE_p is obtained as:

$$\widetilde{W}^{SE}_p = \frac{W^{SE}_p}{1 + W^{SE}_p - R^{SE}_p} \tag{26}$$

where $W^{SE}_p = \frac{\exp\left(SIL\left(SE_p\right)\right)+\exp\left(DEL\left(SE_p\right)\right)}{\sum_{p=1}^{P}\left(\exp\left(SIL\left(SE_p\right)\right)+\exp\left(DEL\left(SE_p\right)\right)\right)}$ and $R^{SE}_p = \frac{1-E\left(SE_p\right)}{P-\sum_{p=1}^{P}E\left(SE_p\right)}$. Here, W^{SE}_p scales initial weight of SE_p, where $SIL\left(SE_p\right) = \frac{\sum_{k=1}^{n_p} SIL\left(dm_{p,k}\right)}{\sum_{p=1}^{P}\sum_{k=1}^{n_p} SIL\left(dm_{p,k}\right)}$, $DEL\left(SE_p\right) = \frac{\sum_{k=1}^{n_p} DEL\left(dm_{p,k}\right)}{\sum_{p=1}^{P}\sum_{k=1}^{n_p} DEL\left(dm_{p,k}\right)}$. R^{SE}_p represents the reliability of SE_p, calculated by average belief entropy $E\left(SE_p\right) = \frac{\sum_{k=1}^{n_p} E\left(dm_{p,k}\right)}{\sum_{p}^{P}\sum_{k=1}^{n_p} E\left(dm_{p,k}\right)}$.

Remark 5. Focus on Eq. (25) and (26), $w^{dm}_{p,k}$ and W^{SE}_p amplifies the influence of differences in DEL and *SIL*, ensuring that even slight variations can significantly impact the weighting. The exponential function here emphasizes more pronounced distinctions among DMs, making it especially sensitive to variations in expertise or domain knowledge.

Definition 16.. (*Normalized DPR matrix*) To ensure consistency, the differences in the multi-granularity frame of discernment should be normalized into a uniform format, $H^* = \{H^*_1, \cdots, H^*_n, \cdots, H^*_N\}$ (N is an odd number). The score value of H^*_n is denoted as $s\left(H^*_n\right)$. The normalized DPR is denoted as $d^{*p,k}_{l,(ij)} = \left\{\left(H^*_n, d^{*p,k}_{l,(ij)}\left(H^*_n\right)\right), n = 1, \cdots, N; \left(H^*, d^{*p,k}_{l,(ij)}\left(H^*\right)\right)\right\}$. For any fine-grained or coarse-grained DPR, the normalization process is defined as:

$$d^{*p,k}_{l,(ij)}\left(H^*_n\right) = d^{\circ p,k}_{l,(ij)}\left(H^*_n\right) + d^{-p,k}_{l,(ij)}\left(H^*_n\right) + d^{+p,k}_{l,(ij)}\left(H^*_n\right) \tag{27}$$

$$\begin{cases} d^{\circ p,k}_{l,(ij)}\left(H^*_n\right) = f^{p,k}_{l,(ij)}\left[(H_n)^{p,k}\right]\left(\text{or } c^{p,k}_{l,(ij)}\left(H^C_n\right)\right) \text{ if } s\left[(H_n)^{p,k}\right]\left(\text{or } s\left(H^C_n\right)\right) = s\left(H^*_n\right) \\ d^{-p,k}_{l,(ij)}\left(H^*_n\right) = \left|\frac{s\left[(H_n)^{p,k}\right]\left(\text{or } s\left(H^C_n\right)\right) - s\left(H^*_{n-1}\right)}{s\left(H^*_n\right) - s\left(H^*_{n-1}\right)}\right| f^{p,k}_{l,(ij)}\left[(H_n)^{p,k}\right]\left(\text{or } c^{p,k}_{l,(ij)}\left(H^C_n\right)\right) \\ \qquad \text{if } s\left[(H_n)^{p,k}\right]\left(\text{or } s\left(H^C_n\right)\right) \in \left[s\left(H^*_{n-1}\right), s\left(H^*_n\right)\right] \\ d^{+p,k}_{l,(ij)}\left(H^*_n\right) = \left|\frac{s\left(H^*_{n+1}\right) - s\left[(H_n)^{p,k}\right]\left(\text{or } s\left(H^C_n\right)\right)}{s\left(H^*_{n+1}\right) - s\left(H^*_n\right)}\right| f^{p,k}_{l,(ij)}\left[(H_n)^{p,k}\right]\left(\text{or } c^{p,k}_{l,(ij)}\left(H^C_n\right)\right) \\ \qquad \text{if } s\left[(H_n)^{p,k}\right]\left(\text{or } s\left(H^C_n\right)\right) \in \left[s\left(H^*_n\right), s\left(H^*_{n+1}\right)\right] \end{cases} \tag{28}$$

Therefore, the independent opinion of each $dm_{p,k}$ with its weight and reliability can be generated by applying ER rule (Yang and Xu, 2013) denoted by F via Eq. (29) for aggregating upper-layer attributes.

$$F\left(\widetilde{W}_1^{p,k}, d^{*p,k}_{1,(ij)}; \cdots; \widetilde{W}_l^{p,k}, d^{*p,k}_{l,(ij)}; \cdots; \widetilde{W}_L^{p,k}, d^{*p,k}_{L,(ij)}\right) = d^{*p,k}_{(ij)}$$
$$(p=1,\cdots,P; k=1,\cdots,n_p; l=1,\cdots,L; i=1,\cdots,M-1; j=i+1,M) \tag{29}$$

Algorithm 2 (I-E responsive multi-granularity evaluating and reweighting algorithm)

Input: Set of Alternatives $X = \{x_1, \dots, x_M\}$; Set of DMs $\{\mathrm{DM}_{(p,k)}\}$; Attributes $A = \{A_1, \dots, A_L\}$ with sub-attributes $a = \{a_{1,1}, \dots, a_{L,n_L}\}$; Normalized frame of discernment $H^* = \{H_1^*, \dots, H_n^*, \dots, H_N^*\}$ (N is odd)

Output: Reweighted attribute weight $\widetilde{W}_l^{(p,k)}$, individual weight $\widetilde{w}_{(p,k)}^{dm}$, group weight $\widetilde{W}_p^{SE}$, normalized DPR $d_{l,(ij)}^{*(p,k)}$

Step 1: Establish I-E Stakeholder Matrix
Calculate $SIL(dm_{(p,k)})$ and $DEL(\mathrm{dm}_{(p,k)})$ for each DM using **Definition 10 and 11**
Determine quadrant placement for each DM using thresholds $\theta_{horizontal}$ and $\theta_{vertical}$ with Eq. (16)

Step 2: Establish Multi-Granularity Preference Model and Normalization
1: Establish Multi-Granularity Preference Model
foreach *DM* **do**
    if $\mathrm{DEL}(\mathrm{dm}_{(p,k)}) \geq \theta_{vertical}$ *and* $\mathrm{dm}_{(p,k)} \in \{\mathrm{IE}^{(H-H)} \vee \mathrm{IE}^{(L-H)}\}$ **then**
        Provide fine-grained DPR matrix using Eq. (17)
    end
    else
        Provide coarse-grained DPR matrix using Eq. (18)
    end
end
2: Normalized DPR matrix
foreach *DM* **do**
    if $s[(H_n)^{(p,k)}] = s(H_n^*)$ *or* $s(H^C) = s(H_n^*)$ **then**
        Use Eq. (28) for normalizing
    end
    if $s[(H_n)^{(p,k)}]$ *or* $s(H^C) \in [s(H_n^*), s(H_{n+1}^*)]$ **then**
        Use Eq. (27) for normalizing
    end
end

Step 3: Reweighting Function for Attributes/Individuals/Entities
Calculate belief entropy on three levels: Attributes/Alternatives/DMs using Eqs. (21)-(23)
Apply entropy-based reweighting to adjust DM influence using Eqs. (24)-(26)

4.2. Decentralized multipartite feedback mechanism for consensus reaching

A decentralized multipartite consensus feedback mechanism incorporating perspectives from various stakeholder entities is designed based on the I-E responsive multi-granularity decision mechanism. Initially, different stakeholder entities are identified as distinct types of DMP. Subsequently, feedback mechanisms are designed to accommodate the specific characteristics of these parties, leading to establishing a multi-objective optimization model aimed at reaching consensus.

4.2.1. Consensus measurement

In the decentralized multipartite feedback mechanism, consensus measurement is essential to initiate further consensus feedback. This step is critical as the decentralized system requires each stakeholder to provide distinct opinions, which serve as reference points for final decision-making.

Definition 17. (*Consensus level between DMs*) Let $d^{*p,k}_{(ij)}$ and $d^{*p,g}_{(ij)}$ be the normalized DPRs on the comparison of alternatives x_i over x_j by $dm_{p,k}$ and $dm_{p,g}$. Then, the consensus level between them is:

$$CL_{kg} = \frac{1}{M-1}\sum\nolimits_{0<i<M-1, j=i+1}\left(1 - diss\left(d^{*p,k}_{(ij)}, d^{*p,g}_{(ij)}\right)\right) \tag{30}$$

Definition 18. (*Consensus level of stakeholder entity*) Suppose there are n_p DMs in stakeholder entity $SE_p = \left\{dm_{p,1}, \cdots, dm_{p,k}, \cdots, dm_{p,n_p}\right\}$. Let $d^{*p,k}_{(ij)}$ be the normalized DPR on the comparison of alternatives x_i over x_j by $dm_{p,k}$. Then, the consensus level of SE_p is calculated by:

$$CL_p = \begin{cases} \dfrac{2}{n_p(n_p-1)}\sum\nolimits_{k=1}^{n_p-1}\sum\nolimits_{g=k+1}^{n_p}\omega_{kg}CL_{kg}, n_p > 1 \\ 1, n_p = 1 \end{cases} \tag{31}$$

where $\omega_{kg} = \frac{\widetilde{w}^{dm}_{p,k}\widetilde{w}^{dm}_{p,g}}{\sum_{k=1}^{n_p-1}\sum_{g=k+1}^{n_p}\widetilde{w}^{dm}_{p,k}\widetilde{w}^{dm}_{p,g}}$ stands for the relative weight of the pairs of $dm_{p,k}$ and $dm_{p,g}$. CL_p is defined by measuring the average preference similarity between each pair of DMs. Let ϖ_p be the accepted consensus level of SE_p, it is obvious that if $CL_p \geq \varpi_p$, SE_p will reach accepted consensus.

4.2.2. Decentralized multipartite consensus feedback mechanism

In the multi-party MAGDM consensus mechanism, the assumptions are: 1) Participant independence: initial opinions from DMs across different stakeholders are independent and uninfluenced by each other. 2) Internal consensus dynamics: participants adjust their decisions by balancing their original views with proposed changes to reach a compromise. Three decision-making participants (DMP) types are identified based on their interactions within the I-E matrix.

a) Non-Consensual Participants: These are stakeholder entities with low interest and expertise. They do not actively participate in the consensus process but their opinions are used as reference. This incorporation ensures that the final decision is balanced, reflecting both the highly engaged expert views and the broader market sentiment of passive stakeholders, which is identified by:

$$DMP^{NC} = \left\{SE_p \middle| \left|\mathrm{IE}^{(L-L)} \cap SE_p\right| \geq \frac{n_p}{3}, p = 1, 2, \cdots, P\right\} \tag{32}$$

Therefore, the opinion of $SE_p \in DMP^{NC}$ is generated by applying F via Eq. (33).

$$d^{*SE_p}_{(ij)} = F\left(\widetilde{w}^{dm}_{p,1}, d^{*p,1}_{(ij)}; \cdots; \widetilde{w}^{dm}_{p,k}, d^{*p,k}_{(ij)}; \cdots; \widetilde{w}^{dm}_{p,n_p}, d^{*p,n_p}_{(ij)}\right)$$
$$(k = 1, \cdots, n_p; i = 1, \cdots, M-1; j = i+1, \cdots, M) \tag{33}$$

If more than one entity belonging to $DMP^{NC}(P > 1)$, then the aggregated DPR of DMP^{NC} will be:

$$d^{*DMP^{NC}}_{(ij)} = F\left(\widetilde{W}^{SE}_p, d^{*SE_p}_{(ij)}; \cdots; \widetilde{W}^{SE}_p, d^{*SE_p}_{(ij)}\right)$$
$$(SE_p \in DMP^{NC}; i = 1, \cdots, M-1; j = i+1, \cdots, M) \tag{34}$$

b) Maximum Return Participants: These stakeholders are identified as being from high-interest regions. They typically do not consider the cost of participation as a barrier and aim for high returns, making them key players in reaching consensus.

$$DMP^{MR} = \left\{SE_p \middle| \left|\left(\mathrm{IE}^{(H-L)} \cup \mathrm{IE}^{(H-H)}\right) \cap SE_p\right| \geq \frac{n_p}{3}, p = 1, 2, \cdots, P\right\} \tag{35}$$

For DMP^{MR}, if $SE_p \in DMP^{MR}$ with $CL_p \geq \varpi_p$, then the collective opinion $d^{*SE_p}_{(ij)}$ of SE_p can be generated by Eq. (33). However, if $CL_p < \varpi_p$, the consensus feedback mechanism will be activated. In CRP, DMs in $SE_p \in DMP^{MR}$ would like to receive more returns. They are motivated to modify their opinions to reach a consensus within the stakeholder entity.

Therefore, focusing on the characteristics of this region, the suggested opinion of $dm_{p,k} \in SE_p \in DMP^{MR}$ can be calculated by

$$\widehat{d}^{*p,k}_{(ij)} = d^{*\{SE_p \cap \mathrm{IE}^{(H-H)}\}}_{(ij)} \tag{36}$$

where $d^{*\{SE_p \cap \mathrm{IE}^{(H-H)}\}}_{(ij)}$ signifies the collective original DPR of $dm_{p,k} \in \{SE_p \cap \mathrm{IE}^{(H-H)}\}$, calculated by:

$$d^{*\{SE_p \cap \mathrm{IE}^{(H-H)}\}}_{(ij)} = F\left(\overline{w}^{dm}_{p,1}, d^{*p,1}_{(ij)}; \cdots; \overline{w}^{dm}_{p,k}, d^{*p,k}_{(ij)}; \cdots; \overline{w}^{dm}_{p,|SE_p \cap \mathrm{IE}^{(H-H)}|}, d^{*p,|SE_p \cap \mathrm{IE}^{(H-H)}|}_{(ij)}\right) \tag{37}$$

where $\overline{w}^{dm}_{p,k} = \frac{\widetilde{w}^{dm}_{p,k}}{\sum_{p=1}^{|SE_p \cap \mathrm{IE}^{(H-H)}|} \widetilde{w}^{dm}_{p,k}}$ represents the average weight of the $dm_{p,k}$ in the set $\{SE_p \cap \mathrm{IE}^{(H-H)}\}$.

On this basis, the objective is to reach a consensus while maximizing their returns. There are two types of the consensus return:

(1) Identification Return (IR). It depends on the collective DPR $\overline{d}^{*SE_p}_{(ij)}$ aggregated by each modified DPR $\overline{d}^{*p,k}_{(ij)}$, which measures how closely an individual's opinion aligns with the collective opinion. This return is influenced by the extent to which a DM's opinion is modified to match the collective view. The IR of $dm_{p,k}$ comes from the following expression:

$$IR_{p,k} = \widetilde{w}^{dm}_{p,k}\left(1 - \sum_{0<i\le M-1, j=i+1} diss\left(\overline{d}^{*p,k}_{(ij)}, \overline{d}^{*SE_p}_{(ij)}\right)\right) \tag{38}$$

where $diss\left(\overline{d}^{*p,k}_{(ij)}, \overline{d}^{*SE_p}_{(ij)}\right)$ measures the dissimilarity between the modified individual opinion $\overline{d}^{*p,k}_{(ij)}$ and collective opinion $\overline{d}^{*SE_p}_{(ij)}$.

(2) Adjustment Return (AR). It depends on the modified DPR $\overline{d}^{*p,k}_{(ij)}$ and the unit reward $\varkappa_{p,k}$, which reflects the extraneous compensation received when an individual is recommended to adjust his/her opinion. The AR of $dm_{p,k}$ can be calculated as:

$$AR_{p,k} = \varkappa_{p,k} \sum_{0<i\le M-1, j=i+1} diss\left(d^{*p,k}_{(ij)}, \overline{d}^{*p,k}_{(ij)}\right) \tag{39}$$

where $diss\left(d^{*p,k}_{(ij)}, \overline{d}^{*p,k}_{(ij)}\right)$ measures the dissimilarity between the modified opinion $\overline{d}^{*p,k}_{(ij)}$ and original opinion $d^{*p,k}_{(ij)}$. DM $dm_{p,k}$ is eligible for external compensation from the moderator only if their modified opinion lies between the original and suggested opinions. And $\varkappa_{p,k}$ can be calculated by

$$\varkappa_{p,k} = \widetilde{w}^{dm\frac{\varpi_p}{CL_{k,DMP^{NC}}}}_{p,k} \tag{40}$$

where $CL_{k,DMP^{NC}}$ represents the consensus level between $d^{*p,k}_{(ij)}$ and $d^{*DMP^{NC}}_{(ij)}$. It is noted that the higher weight of $dm_{p,k}$ will lead to higher reward $\varkappa_{p,k}$ for the $dm_{p,k}$. When $CL_{k,DMP^{NC}} > \varpi_p$, $\frac{\varpi_p}{CL_{k,DMP^{NC}}} < 1$, we have $\varkappa_{p,k} > \widetilde{w}^{dm}_{p,k}$ which means that if the opinion of $dm_{p,k}$ is closer to the non-consensual participants, he/she will receive more unit rewards and vice versa.

It is obvious that $IR_{p,k}, AR_{p,k} \in [0,1]$. According to Eq. (38)-(39), the total return of SE_p is:

$$UR_p = \sum_{k=1}^{n_p} \left(IR_{p,k} + AR_{p,k}\right) \tag{41}$$

Then, the optimization model regarding $SE_p \in DMP^{MR}$ can be constructed as a Model I:

Model I : $\max UR_p$

$$s.t.\begin{cases} CL_p = \dfrac{2}{n_p(n_p-1)} \sum_{k=1}^{n_p-1} \sum_{g=k+1}^{n_p} \omega_{kg} CL_{kg} \ge \varpi_p \\ CL_{kg} = \dfrac{1}{M-1} \sum\limits_{0<j=i+1<M}^{0<i\le M-1} \left(1 - diss\left(d^{*p,k}_{(ij)}, d^{*p,g}_{(ij)}\right)\right) \\ diss\left(d^{*p,k}_{(ij)}, d^{*p,g}_{(ij)}\right) = \dfrac{1}{2} \sum_{n=1}^{N-1} \sum_{n'=n+1}^{N} \psi^{kg}_{ij}(H_n) \psi^{kg}_{ij}(H_{n'}) (s((H_{n'})) - s(H_n)) \\ \psi^{kg}_{ij}(H_n) = \left| d^{*p,k}_{(ij)}(H_n) - d^{*p,g}_{(ij)}(H_n) \right| \\ \overline{d}^{*p,k}_{(ij)} = (1 - \varrho_{p,k}) d^{*p,k}_{(ij)} + \varrho_{p,k} \widehat{d}^{*p,k}_{(ij)} \\ \widehat{d}^{*p,k}_{(ij)} = d^{*\{SE_p \cap IE^{(H-H)}\}}_{(ij)} \\ d^{*\{SE_p \cap IE^{(H-H)}\}}_{(ij)} = F\left(\overline{w}^{dm}_{p,1}, d^{*p,1}_{(ij)}; \cdots; \overline{w}^{dm}_{p,k}, d^{*p,k}_{(ij)}; \cdots; \overline{w}^{dm}_{p,|SE_p \cap IE^{(H-H)}|}, d^{*p,|SE_p \cap IE^{(H-H)}|}_{(ij)}\right) \\ \varkappa_{p,k} = \widetilde{w}^{dm\frac{\varpi_p}{CL_{k,DMP^{NC}}}}_{p,k} \\ CL_{k,DMP^{NC}} = \dfrac{1}{M-1} \sum\limits_{0<j=i+1<M}^{0<i\le M-1} \left(1 - diss\left(d^{*p,k}_{ij}, d^{*DMP^{NC}}_{(ij)}\right)\right) \\ d^{*DMP^{NC}}_{(ij)} = F\left(\widetilde{W}^{SE}_p, d^{*SE_p}_{(ij)}; \cdots; \widetilde{W}^{SE}_p, d^{*SE_p}_{(ij)}\right) \left(SE_p \in DMP^{NC}; i = 1, \cdots, M-1; j = i+1\right) \\ \overline{d}^{*SE_p}_{(ij)} = F\left(\widetilde{w}^{dm}_{p,1}, \overline{d}^{*p,1}_{(ij)}; \cdots; \widetilde{w}^{dm}_{p,k}, \overline{d}^{*p,k}_{(ij)}; \cdots; \widetilde{w}^{dm}_{p,n_p}, \overline{d}^{*p,n_p}_{(ij)}\right) \\ dm_{p,k} \in SE_p \in DMP^{MR} \\ \varrho_{p,k} \in [0,1] \end{cases} \tag{42}$$

As shown in **Model I**, the decision variables $\varrho_{p,k}$ affects the value of the objective function and determines the final DPR matrix of each DM in $SE_p \in DMP^{MR}$ under acceptable consensus level constraints. $\overline{d}^{*p,k}_{(ij)}$ and $\overline{d}^{*SE_p}_{(ij)}$ are the final modified DPR of $dm_{p,k}$ and SE_p under the optimal $\varrho_{p,k}$.

c) Minimum Cost Participants: From the low-interest and high-expertise region. These DMP aim to achieve consensus with the least possible cost, focusing on efficiency over extensive involvement.

$$DMP^{MC} = \left\{ SE_p \middle| \left| \mathrm{IE}^{(L-H)} \cap SE_p \right| \geq \frac{n_p}{3}, p = 1, 2, \cdots, P \right\} \tag{43}$$

If $SE_p \in DMP^{MC}$ with $CL_p \geq \varpi_p$, then the collective opinion $d^{*SE_p}_{(ij)}$ can be generated by Eq. (33). However, if $CL_p < \varpi_p$, the consensus feedback mechanism will be activated. In this scenario, DMs in $SE_p \in DMP^{MC}$ are more inclined to accept proposals that align closely with collective preferences, aiming to minimize costs for achieving consensus. They prefer adopting suggestions that favor a group consensus, thereby reducing the efforts needed to persuade stakeholders to alter their views. Therefore, based on these characteristics, the suggested opinion of $dm_{p,k} \in SE_p \in DMP^{MC}$ can be calculated by

$$\widehat{d}^{*p,k}_{(ij)} = d^{*\left\{SE_p \cap \mathrm{IE}^{(L-H)}\right\}}_{(ij)} \tag{44}$$

where $d^{*\left\{SE_p \cap \mathrm{IE}^{(L-H)}\right\}}_{(ij)}$ stands for the collective original DPR of $dm_{p,k} \in \left\{SE_p \cap \mathrm{IE}^{(l-H)}\right\}$ which is:

$$d^{*\left\{SE_p \cap \mathrm{IE}^{(L-H)}\right\}}_{(ij)} = F\left(\overline{w}^{dm}_{p,1}, d^{*p,1}_{(ij)}; \cdots; \overline{w}^{dm}_{p,k}, d^{*p,k}_{(ij)}; \cdots; \overline{w}^{dm}_{p,\left|SE_p \cap \mathrm{IE}^{(L-H)}\right|}, d^{*p,\left|SE_p \cap \mathrm{IE}^{(L-H)}\right|}_{(ij)}\right) \tag{45}$$

where $\overline{w}^{dm}_{p,k} = \frac{\widetilde{w}^{dm}_{p,k}}{\sum_{p=1}^{\left|SE_p \cap \mathrm{IE}^{(L-H)}\right|} \widetilde{w}^{dm}_{p,k}}$ represents the average weight of $dm_{p,k}$ in the set $\left\{SE_p \cap \mathrm{IE}^{(L-H)}\right\}$.

Here, the objective is to reach consensus with the minimum cost. Similar to the external compensation strategy of AR for DMP^{MR}, the consensus cost (CC) for $dm_{p,k}$ within $SE_p \in DMP^{MC}$ can be seen as the effort required to persuade a DM to change opinion, which can be calculated by:

$$CC_{p,k} = c_{p,k} \sum_{0<i\leq M-1, j=i+1} \left(diss\left(d^{*p,k}_{(ij)}, \overline{d}^{*p,k}_{(ij)} \right) \right) \tag{46}$$

where the unit consensus cost is given by

$$c_{p,k} = \widetilde{w}^{dm}_{p,k} \tag{47}$$

Then, the optimization model regarding $SE_p \in DMP^{MC}$ is constructed as Model II:

$$\text{Model II}: \min CC_p = \sum\nolimits_{k=1}^{n_p} \left(c_{p,k} \sum\nolimits_{0<i\leq M-1, j=i+1} \left(diss\left(d^{*p,k}_{(ij)}, \overline{d}^{*p,k}_{(ij)} \right) \right) \right)$$

$$s.t. \begin{cases} CL_p = \dfrac{2}{n_p(n_p-1)} \sum\nolimits_{k=1}^{n_p-1} \sum\nolimits_{g=k+1}^{n_p} \omega_{kg} CL_{kg} \geq \varpi_p \\ CL_{kg} = \dfrac{1}{M-1} \sum\limits_{0<j=i+1<M}^{0<i\leq M-1} \left(1 - diss\left(d^{*p,k}_{(ij)}, d^{*p,g}_{(ij)} \right) \right) \\ diss\left(d^{*p,k}_{(ij)}, d^{*p,g}_{(ij)} \right) = \dfrac{1}{2} \sum\nolimits_{n=1}^{N-1} \sum\nolimits_{n'=n+1}^{N} \psi^{kg}_{ij}(H_n) \psi^{kg}_{ij}(H_{n'}) (s(H_{n'}) - s(H_n)) \\ \psi^{kg}_{ij}(H_n) = \left| d^{*p,k}_{(ij)}(H_n) - d^{*p,g}_{(ij)}(H_n) \right| \\ \overline{d}^{*p,k}_{(ij)} = (1 - \varrho_{p,k}) d^{*p,k}_{(ij)} + (\varrho_{p,k}) \widehat{d}^{*p,k}_{(ij)} \\ \widehat{d}^{*p,k}_{(ij)} = d^{*SE_p}_{(ij)} \\ d^{*SE_p}_{(ij)} = F\left(\widetilde{w}^{dm}_{p,1}, d^{*p,1}_{(ij)}; \cdots; \widetilde{w}^{dm}_{p,k}, d^{*p,k}_{(ij)}; \cdots; \widetilde{w}^{dm}_{p,n_p}, d^{*p,n_p}_{(ij)} \right) \\ c_{p,k} = \widetilde{w}^{dm}_{p,k} \\ dm_{p,k} \in SE_p \in DMP^{MC} \\ \varrho_{p,k} \in [0,1] \end{cases} \tag{48}$$

As shown in Model II, the decision variables $\varrho_{p,k}$ affects the value of objective function and determine the final DPR matrix of DM in $SE_p \in DMP^{MC}$ under acceptable consensus level constraint. Therefore, the optimized collective DPR matrix of SE_p can be obtained after adjustment.

Remark 6. The consensus optimization models (Model I for maximum return and Model II for minimum cost) are formulated over the adjustment variables $\rho \in [0,1]^{n_p}$. The Weierstrass Extreme Value Theorem guarantees an optimal solution since the feasible region is a compact set and the objective functions, including the identification and adjustment returns, are continuous in Rho. Furthermore, if the overall objective function is strictly convex, the optimal solution is unique if its Hessian is positive and definite over the feasible set's interior. In our model, the decision variable ρ enters through an affine transformation of the original DPR matrices, and the dissimilarity functions (constructed from absolute differences) are convex. However, due to exponential weighting in the adjustment return, strict convexity may not always hold; hence, multiple local optima are theoretically possible. To address this, we solve the model using the sequential least squares programming (SLSQP) algorithm, which iteratively approximates the nonlinear objective and constraints by quadratic and linear models, respectively. In cases where the aim is nonconvex, multiple initializations are employed to improve the likelihood of finding the global optimum. This approach ensures the model to produce a solution that satisfies the consensus constraints and is a reliable output for our decision-making process.

4.2.3. *Decentralized multipartite consensus reaching process*

Based on the design of the I-E responsive multi-granularity decision model and feedback mechanism, we construct the decentralized multipartite consensus algorithm, as shown in Algorithm 3. In the feedback adjustment process, stakeholder entities are first categorized into three groups based on their I-E attributes: non-consensual participants (DMP^{NC}), Maximum Return Participants (DMP^{MR}), and Minimum Cost Participants (DMP^{MC}). For entities in DMP^{MR}, if the initial consensus level CL_p is below the accepted threshold ϖ_p, Model I is applied to iteratively adjust individual opinions to maximize the identification and adjustment return. Similarly, for entities in DMP^{MC}, Model II is employed to minimize the consensus cost under the same consensus constraint. These optimization processes are executed independently, ensuring that the adjustment of opinions in one group does not affect that in the other. After convergence within each group, the optimized opinions are aggregated via the decentralized consensus algorithm to yield the final collective decision. After each entity completes the CRP, the optimal DPR matrix that meets the acceptable consensus level is generated. The next step involves selecting the final ranking of alternatives. Entities' opinions are then fused using Eq. (49) for optimal decisions. The complete process is depicted in Fig. 6.

$$F\left(\widetilde{W}_1^{SE}, \overline{d}_{(ij)}^{*SE_1}; \cdots; \widetilde{W}_p^{SE}, \overline{d}_{(ij)}^{*SE_p}; \cdots; \widetilde{W}_P^{SE}, \overline{d}_{(ij)}^{*SE_P}\right) = \overline{d}_{(ij)}^{*C} \quad (p = 1, \cdots, P; i = 1, \cdots, M-1; j = i+1, \cdots, M) \tag{49}$$

Algorithm 3 (Decentralized multipartite consensus reaching algorithm)

Input: Set of stakeholder entities $SE = \{SE_1, \ldots, SE_P\}$ $(P \geq 2)$; DMs' preferences $d_{l,(ij)}^{*(p,k)}$; reweighted weights $\widetilde{W}_l^{p,k}, \widetilde{w}_{p,k}^{dm}, \widetilde{W}_p^{SE}$; consensus threshold ϖ_p
Output: Final ranking of alternatives, collective DPR matrix
Step 1: Consensus Measurement
For each pair of DMs within a stakeholder entity, calculate initial consensus levels using **Definition 17**
Step 2: Decentralized Multipartite Consensus Feedback Mechanism
foreach SE_p **do**
  if $|\mathrm{IE}^{(L-L)} \cap SE_p| \geq \frac{n_p}{3}$ **then**
    $SE_p \in \mathrm{DMP}^{NC}$
    The opinion of SE_p is generated by Eq. (33)
  end
  else if $(|\mathrm{IE}^{(H-L)} \cup \mathrm{IE}^{(H-H)}) \cap SE_p| \geq \frac{n_p}{3}$ **then**
    $SE_p \in \mathrm{DMP}^{MR}$
    Calculate the internal consensus level CL_p for SE_p using **Definition 18**
    if $CL_p \geq \varpi_p$ **then**
      Fuse all DPRs of DMs by Eq. (33)
    end
    else
      Apply Maximum Return Optimization **Model I**
    end
  end
  else if $|\mathrm{IE}^{(L-H)} \cap SE_p| \geq \frac{n_p}{3}$ **then**
    $SE_p \in \mathrm{DMP}^{MC}$
    Calculate the internal consensus level CL_p for SE_p using **Definition 18**
    if $CL_p \geq \varpi_p$ **then**
      Fuse all DPRs of DMs by Eq. (33)
    end
    else
      Apply Minimum Cost Optimization **Model II**
    end
  end
end
Step 3: Decentralized Multipartite Selecting Process
forall SE_p **do**
  Apply Eq. (49) for generating the final collective opinion $\vec{d}_{(ij)}^{*C}$ of multipartite
end
Select the optimal alternative by score matrix $S_C = ([S_{ij}^{(C)-}, S_{ij}^{(C)+}])_{M\times M}$ and PD matrix $PD_C = (pd_{ij}^{C})_{M\times M}$

5. Illustrative example and comparison

This section describes a case study in an NEV R&D department to illustrate the practical use of methodologies from prior chapters. It explores the intricate product development lifecycle in the NEV industry, focusing on the essential concept evaluation stage. We demonstrate alignment with user preferences and technological standards by implementing the suggested decentralized multipartite feedback mechanism and consensus model. Comparative analysis with other GDM methods, particularly on UGC, shows the effectiveness of our approach. Moreover, sensitivity analyses of the optimization models reveal their robustness and adaptability in diverse scenarios.

5.1. An illustrative example of new energy vehicle R&D

5.1.1. Case description

In today's fast-changing technological environment, strategic industries like NEVs are crucial for reshaping global economies and addressing environmental issues. NEV's success hinges on technological progress and meeting consumer preferences and experiences. The product development cycle includes seven phases: concept, detailed development, debugging, release, iteration, and obsolescence. The first phase is concept design, which involves generating and evaluating potential designs. Practical concept evaluation can lead to disruptive innovations and considerable success, while poor evaluation can increase costs, extend development time, require additional revisions, and heighten project uncertainty. Concept evaluation's importance in subsequent stages highlights its role in the design process, necessitating a comprehensive analysis of technological progress, design constraints, and user satisfaction. This paper explores a decentralized multipartite consensus model for MAGDM, focusing on user experience within NEV R&D. We offer an example with a set of medium-sized SUV R&D alternatives $X = \{x_1, x_2, \cdots, x_5\}$, selected based on UGC data, as illustrated in Fig. 7.

Contrary to a purely theoretical model, our approach is grounded in authentic UGC from historical NEV customer reviews, as partially illustrated in Fig. 8. Based on these time-efficient UGC, a two-layer UXO attribute system $A = \{A_1, \cdots, A_L\} = \{a_{1,1}, \cdots, a_{1,n_1}; \cdots; a_{L,1}, \cdots, a_{L,n_L}\} (L \geq 2, n_l \geq 1)$ with weights $w = \{w_{1,1}, \cdots, w_{1,n_1}; \cdots; w_{L,1}, \cdots, w_{L,n_l}\}$ could be established by applying Algorithm 1, which detailed in Section 5.1.2. To improve customer satisfaction and economic returns post-launch, the selection of R&D alternatives should incorporate evaluations from multiple stakeholders. The R&D department has extended invitations to DMs from three distinct stakeholder entities, $SE = \{SE_1, SE_2, SE_3\}$, which includes **internal experts** (from NEV R&D department), **external experts** (from university, institute, third-party engineer), and **target users.**

5.1.2. Construct evaluation attributes system

Step 1. UGC data acquisition and domain-specific corpus construction. In order to harness the wealth of unstructured UGC, we deploy an advanced database generator to systematically collect data across an automobile review platform (*pcauto.com.cn*). This automated tool targets new, energetic, medium-sized SUV-related discussions, reviews, and feedback. The raw data is segmented into individual words and anonymized to protect user identity, and irrelevant or redundant information is removed. The resulting domain-specific corpus was a foundational dataset from which user experience attributes are derived. Quality metrics calculated by Eq. (4) are applied to the corpus, ensuring the relevance and accuracy of the data. The information on domain-specific corpus is detailed in Table 2. The whole process in this step could be implemented following Module 1 of Algorithm 1.

Step 2. Large-scale sentence embedding. Leveraging the pre-processed corpus, we employ an SBERT model, optimized with *SSRcos* loss function defined in Definition 5 to generate embeddings. This approach generates large-scale sentence embeddings that transform textual data into a standard 768-dimensional vector space for BERT-based models. Our dataset, containing 199,601 reviews, the resulting embedding matrix size was (199601, 768). Each row in this matrix

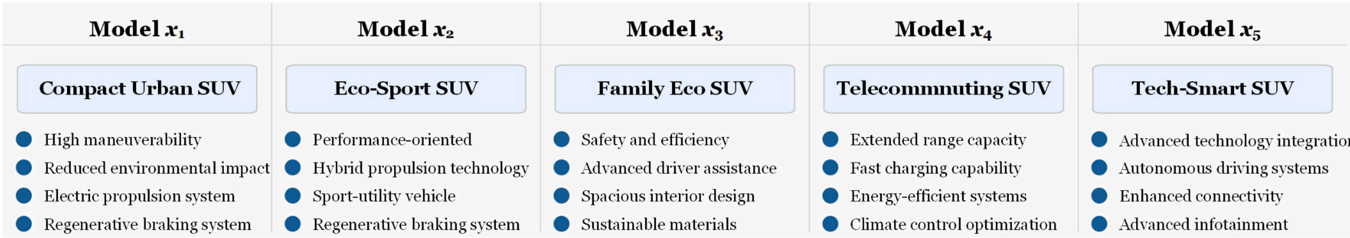

Fig. 7. Medium-sized SUV R&D alternatives.

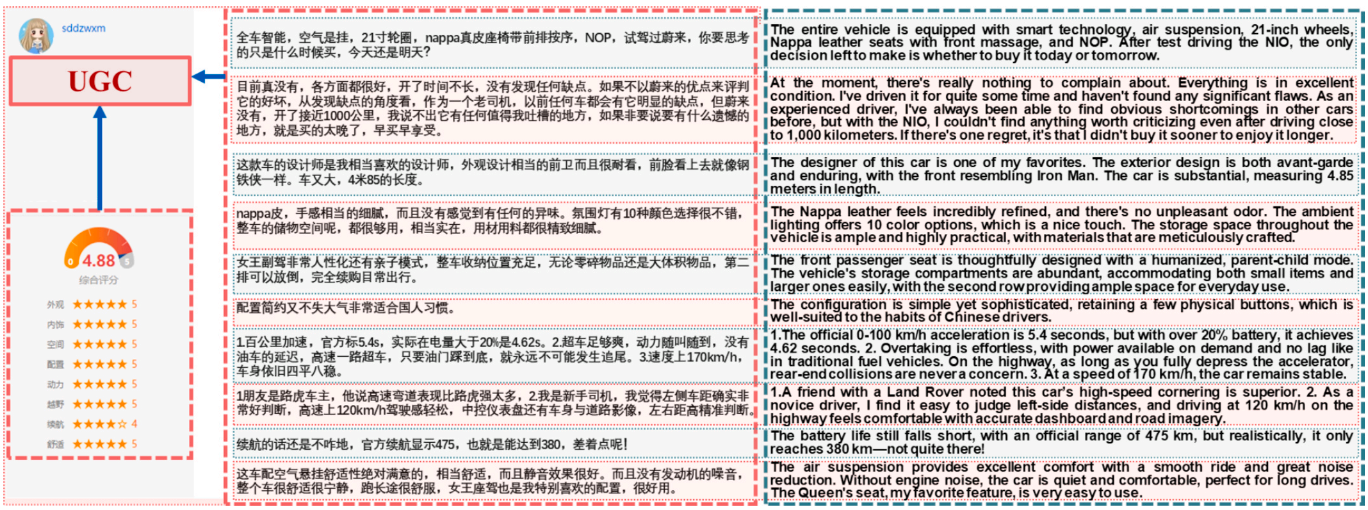

Fig. 8. An example of UGC from a historical customer.

Table 2
Domain-specific corpus information.

Data source	The number of brands	The number of series	The number of reviews
pcauto.com.cn	38	53	199,601

corresponds to a vector representation of a user review, encapsulating semantic depth and intricacies of user opinions. The whole process in this step could be implemented following Module 2 of Algorithm 1.

Step 3. Attributes clustering and discovery. By employing UMAP-assisted HDBSCAN, we compact the data's dimensionality and discern distinct sentence clusters, maintaining local and global structural integrity. We fine-tune hyperparameters through a comprehensive grid search, whose efficacy is rigorously assessed via SC, D-B Score, and C-H Score. Fig. 9 depicts the iterative optimization process, while Table 3 shows the best balance among neighbor count, reduced dimensionality, and minimal cluster size. The whole process in this step could be implemented following Module 3 of Algorithm 1.

Step 4. Attribute integration and weight distribution. Before constructing the UXO attribute system, we employ a two-stage process to assess the significance of clustered attributes in capturing user preferences: a Count Vectorizer converts text into feature vectors, followed by an A-TF-IDF transformation as described in Definition 6. This highlights the significance of domain-specific terms across attribute clusters. We then streamline the attribute sets using the algorithm from Module 4 of Algorithm 1. The process is iterative, visualized in Fig. 10, with Table 3 detailing the aggregation iterations and the final attribute set count. A similarity matrix is created between attribute sets based on

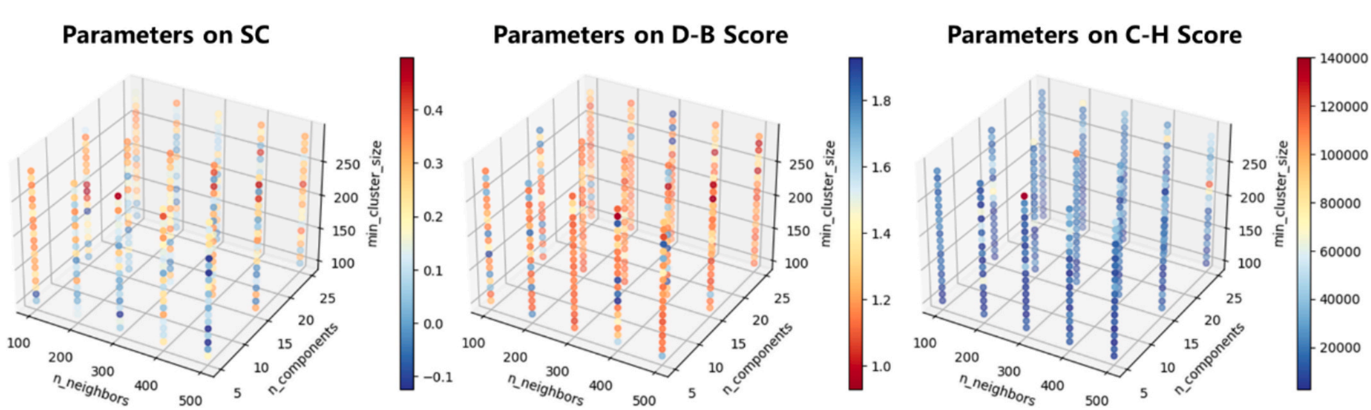

Fig. 9. Grid search process based on three benchmark metrics.

Table 3
Hyperparameter setting and cluster aggregation under optimal benchmark metrics.

Benchmark metrics	SC	D-B Score	C-H Score
The number of neighboring	100	500	300
The dimensionality after reducing	15	15	5
The minimum size of a cluster	200	260	290
The number of optimal clusters	41	21	32
The number of aggregation iterations	35	13	24
The number of clusters after aggregation	6	8	8

Definition 7 and the optimal hyperparameter settings of three benchmark metrics, shown in Fig. 10 panels (a1)-(a3). This matrix establishes a baseline for attribute relatedness at iteration = 0. Through multiple iteration rounds, the matrix updates to reflect attribute convergence into fewer clusters. We apply the optimal benchmark metrics to finalize the clusters upon meeting the convergence criteria in Eq. (9). Panels (b1)-(b3) of Fig. 10 show the evolving similarity matrix, and panels (c1)-(c3) display the final 2-D representations, chosen for their explicit depiction of clustering outcomes. Table 4 and Fig. 11 present the final aggregation and weight distribution results.

In NEV R&D, acquiring extensive user experience data is vital for aligning designs with consumer preferences. The proposed automated method for large-scale corpus acquisition and attribute system construction avoids experientialism. By leveraging data mining technologies, it integrates real-world feedback, enhancing R&D responsiveness to evolving consumer demands and technological advances.

5.1.3. *Apply the proposed method for ranking alternatives*

In the following phases, 20 DMs from $SE = \{SE_1, SE_2, SE_3\}$ will

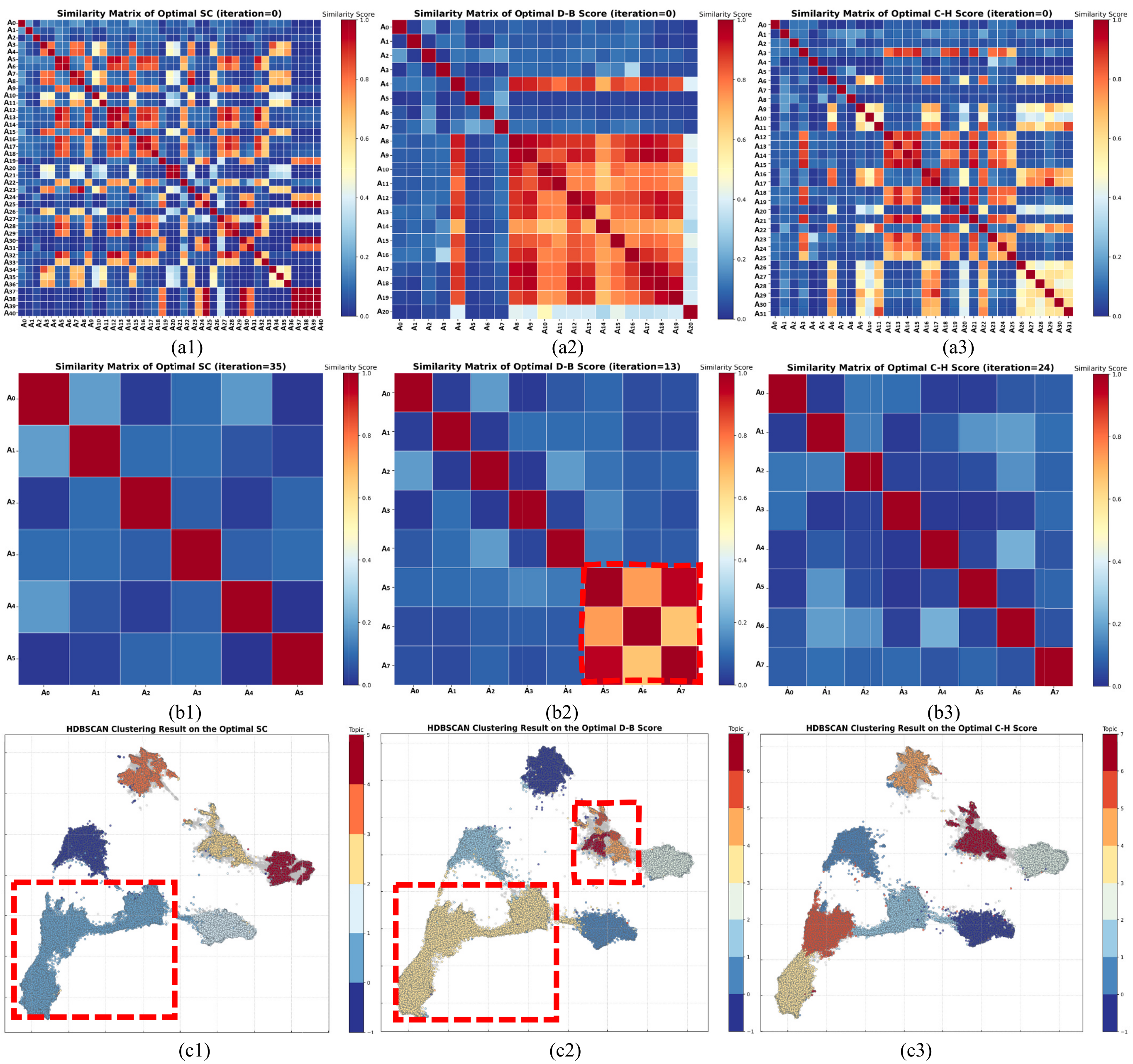

Fig. 10. The iteration process of attribute aggregation. (a1)–(a3) represent the similarity matrix of three benchmark metrics before aggregation (iteration = 0); (b1)–(b3) represent the similarity matrix of three benchmark metrics after multiple rounds of iteration aggregation; (c1)–(c3) represent the final result on three optimal benchmark metrics (n_components = 2 for showing in 2-D).

Table 4
UXO attribute system with relative weights.

A_l	W_l	$a_{l,i}$	$w_{l,i}$	A_l	W_l	$a_{l,i}$	$w_{l,i}$
Power	0.135	Engine	0.242	Interior	0.138	Design	0.195
		Accelerator	0.162			Materials	0.252
		Ride	0.139			Futuristic	0.104
		Speed	0.131			Smell	0.099
		Mode	0.095			Style	0.094
		Electromotor	0.080			Functionality	0.087
		Gearbox	0.077			Center Console	0.086
		Gradeability	0.074			Screen	0.083
Console	0.153	Steering Wheel	0.268	Space	0.158	Trunk	0.293
		Brake	0.149			Rear	0.237
		Chassis	0.131			Stowage	0.136
		Assistance	0.114			Seat	0.108
		Precision	0.099			Head	0.079
		Functionality	0.087			Comfort	0.052
		Sensitive	0.078			Distance	0.048
		Body rigidity	0.074			Space Design	0.047
Endurance	0.129	Fuel Economy	0.700	Appearance	0.070	Appearance Design	0.482
		Hybrid	0.063			Head Lamp	0.128
		Energy Economy	0.102			Body Lines	0.107
		Breaking-in Period	0.050			Styling	0.104
		Economy	0.043			Body	0.094
		Mode	0.043			Tail Lamp	0.085
Configuration	0.097	Performance-Price Ratio	0.360	Comfort	0.120	Seat	0.349
		Price	0.258			Insulation	0.398
		Maintenance	0.102			Air Conditioner	0.124
		Brand	0.073				
		Keep Value	0.068			Seat Adjustment	0.065
		Characteristic	0.050				
		Model	0.045			Shock Absorber	0.065
		Quality	0.044				

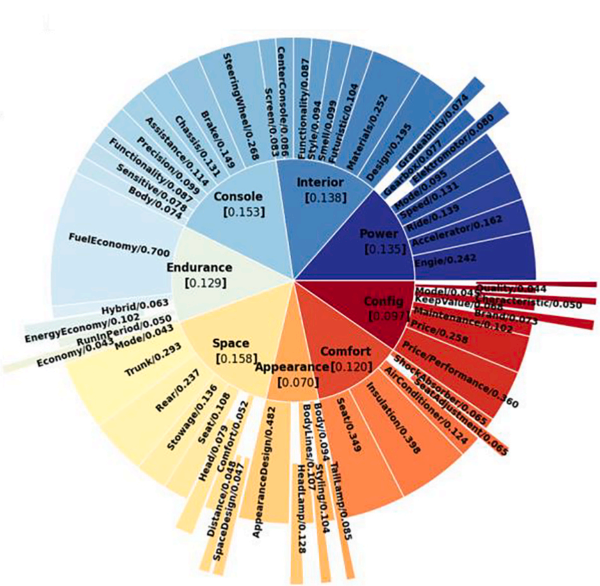

Fig. 11. UXO attribute system with relative weights distribution result.

evaluate 5 R&D alternatives by their own preference model and reach consensus for selecting optimal solution.

Phase 1: Apply Algorithm 2 for obtaining the evaluation of each DM from $\{SE_1, SE_2, SE_3\}$ ***as well as relative weights of attributes and DMs.***

Step 1: Establish I-E matrix. First, $SIL(dm_{p,k})$ and $DEL(dm_{p,k})$ of each DM are calculated by **Definitions 10 and 11**. The value of $SIL(dm_{p,k})$ can be directly calculated as **Example 1**, while the value of $DEL(dm_{p,k})$ partly depends on the PTS of other DMs in the inner stakeholder entity, which are shown in Table 5. Besides, the whole calculating details are shown in Table 6, which can refer to Supplementary Materials' Part A. Based on them, the predefined $\gamma' = \delta' = 0$ so that $\theta_{horizontal} = \mu_{SIL} = 0.70$ and $\theta_{vertical} = \mu_{DEL} = 0.73$. Therefore, each DM can be identified into different I-E region which is presented in Fig. 12.

Step 2: Establish a multi-granularity preference model and normalization. Following **Step 1**, as Fig. 12, the DMs who should provide fine-grained DPRs by Eq. (17) include $dm_{1,1}, dm_{1,2}, dm_{1,3}, dm_{2,1}$, $dm_{2,3}$ and $dm_{2,4}$. Other DMs should give coarse-grained DPRs by Eq. (18). The detailed initial DMs' preferences are shown in Supplementary Materials (Part B for fine-grained DPRs and Part C for coarse-grained DPRs). Here, we give two examples for displaying the DPRs generation process of $dm_{1,1}$ and $dm_{2,2}$. For $dm_{1,1}$, the frame of discernment for evaluating alternatives is $H^{1,1} = \left\{(H_1)^{1,1}, \cdots, (H_9)^{1,1}\right\}$, and $s^{1,1} = \{-1, -0.75, -0.5, -0.25, 0, 0.25, 0.5, 0.75, 1\}$. Based on the initial evaluation on A_1 given by $dm_{1,1}$, the fine-grained DPRs are obtained by Eq. (17) and the entropy can be calculated by Eq. (19). In this case, the normalized frame of discernment is $H^* = \{H_1^*, \cdots, H_5^*\}$, then $d_{l,(ij)}^{p,k}$ can be normalized into $d_{l,(ij)}^{*p,k}$ by Eqs. (28–27). The detailed calculation process of $dm_{1,1}$'s fine-grained DPRs on A_1 are shown in Table 7. For $dm_{2,2}$, the evaluation on A_l is based on $H^C = \{H_1^C, \cdots, H_5^C\}$ with $s^C = \{-1, -0.5, 0, 0.5, 1\}$, which equals to the normalized frame of discernment. DMs such as $dm_{2,2}$ just need to offer direct DPRs for evaluating alternatives. Table 8 shows the initial assessment of $dm_{2,2}$ for evaluating A_1 and the entropy can be calculated by Eq. (20). After applying this step, the normalized DPRs $d_{l,(ij)}^{*p,k}$ of each DM can be finally obtained.

Step 3: Updating the weights of attributes/individuals/entities by reweighting the function. In this step, we apply the reweighting function to update the relative weights of attributes/individuals/entities based on the original weights and the reliability of the assessment. Based on **Definitions 14 and 15**, the average belief entropy on three levels, attributes/alternatives/DMs, can be calculated by Eqs. (21–23). According to the belief entropy of the initial assessment, we update the weights of upper attributes, DMs, and entities by Eqs. (24–26). The reweighted results of individuals and entities are shown in Table 9.

In NEV R&D, the reweighted attribute and stakeholder weights method incorporates subjective preferences and uncertainties, which is

Table 5
Peer-reviewed trust score of each DM.

$dm_{1,k}$	$dm_{1,1}$			$dm_{1,2}$			$dm_{1,3}$			$dm_{1,4}$			$dm_{1,5}$		
	t_{kh}	d_{kh}	ts_{kh}	t_{kh}	d_{kh}	ts_{kh}	t_{kh}	d_{kh}	ts_{kh}	t_{kh}	d_{kh}	ts_{kh}	t_{kh}	d_{kh}	ts_{kh}
$dm_{1,1}$	–			0.70	0.10	0.80	0.80	0.20	0.80	0.60	0.20	0.70	0.50	0.40	0.55
$dm_{1,2}$	0.80	0.10	0.85	–			0.70	0.10	0.80	0.50	0.20	0.65	0.40	0.50	0.45
$dm_{1,3}$	0.90	0.00	0.95	0.70	0.20	0.75	–			0.60	0.30	0.65	0.60	0.40	0.60
$dm_{1,4}$	0.80	0.00	0.90	0.60	0.20	0.70	0.80	0.10	0.85	–			0.50	0.40	0.55
$dm_{1,5}$	0.90	0.10	0.90	0.80	0.10	0.85	0.70	0.10	0.80	0.70	0.20	0.75	–		
$PTS_{p,k}$	0.90			0.78			0.81			0.68			0.53		
$dm_{2,k}$	$dm_{2,1}$			$dm_{2,2}$			$dm_{2,3}$			$dm_{2,4}$			$dm_{2,5}$		
	t_{kh}	d_{kh}	ts_{kh}	t_{kh}	d_{kh}	ts_{kh}	t_{kh}	d_{kh}	ts_{kh}	t_{kh}	d_{kh}	ts_{kh}	t_{kh}	d_{kh}	ts_{kh}
$dm_{2,1}$	–			0.60	0.30	0.65	0.80	0.20	0.80	0.60	0.20	0.70	0.50	0.40	0.55
$dm_{2,2}$	0.80	0.10	0.85	–			0.90	0.00	0.95	0.50	0.20	0.65	0.40	0.50	0.45
$dm_{2,3}$	0.70	0.00	0.85	0.50	0.40		–			0.60	0.30	0.65	0.70	0.20	0.75
$dm_{2,4}$	0.60	0.20	0.70	0.70	0.20	0.75	0.80	0.10	0.85	–			0.50	0.40	0.55
$dm_{2,5}$	0.90	0.10	0.90	0.60	0.20	0.70	0.90	0.10	0.90	0.90	0.10	0.90	–		
$PTS_{p,k}$	0.83			0.53			0.875			0.725			0.575		

Table 6
I-E matrix calculation process.

SE_p	$dm_{p,k}$	$SIL(dm_{p,k})$				$DEL(dm_{p,k})$			$w_{p,k}^{dm}$	W_p^{SE}
		$\gamma_1 = 0.40$ ROI	$\gamma_2 = 0.40$ SEL	$\gamma_3 = 0.20$ IVS	SUM SIL	$\delta_1 = 0.70$ PTS	$\delta_2 = 0.30$ KDI	SUM DEL		
SE_1	$dm_{1,1}$	0.80	0.82	0.9	**0.83**	0.90	0.99	**0.93**	0.238	0.382
	$dm_{1,2}$	0.78	0.68	0.8	**0.74**	0.78	0.80	**0.78**	0.206	
	$dm_{1,3}$	0.88	0.78	0.9	**0.84**	0.81	0.57	**0.74**	0.198	
	$dm_{1,4}$	0.65	0.57	0.6	0.61	0.69	0.50	0.63	0.177	
	$dm_{1,5}$	0.52	0.44	0.6	0.50	0.54	0.90	0.65	0.180	
SE_2	$dm_{2,1}$	0.25	0.34	0.2	0.27	0.83	0.98	**0.87**	0.225	0.344
	$dm_{2,2}$	0.33	0.48	0.6	0.44	0.53	0.80	0.61	0.173	
	$dm_{2,3}$	0.28	0.65	0.6	0.49	0.88	0.95	**0.90**	0.231	
	$dm_{2,4}$	0.65	0.78	0.5	0.67	0.73	0.75	**0.73**	0.196	
	$dm_{2,5}$	0.78	0.68	0.5	0.68	0.58	0.70	0.61	0.174	
SE_3	$dm_{3,1}$	0.12	0.21	0.5	0.23	0.00	0.80	0.24	0.113	0.274
	$dm_{3,2}$	0.09	0.11	0.1	0.10	0.00	0.40	0.12	0.100	
	$dm_{3,3}$	0.11	0.23	0.3	0.20	0.00	0.20	0.06	0.094	
	$dm_{3,4}$	0.10	0.12	0.10	0.11	0.00	0.15	0.05	0.093	
	$dm_{3,5}$	0.20	0.15	0.3	0.20	0.00	0.35	0.11	0.099	
	$dm_{3,6}$	0.68	0.55	0.7	0.63	0.00	0.45	0.14	0.102	
	$dm_{3,7}$	0.18	0.23	0.5	0.26	0.00	0.23	0.07	0.095	
	$dm_{3,8}$	0.34	0.78	0.7	0.60	0.00	0.15	0.05	0.093	
	$dm_{3,9}$	0.17	0.21	0.2	0.19	0.00	0.33	0.10	0.098	
	$dm_{3,10}$	0.75	0.56	0.8	0.68	0.00	0.78	0.23	0.112	

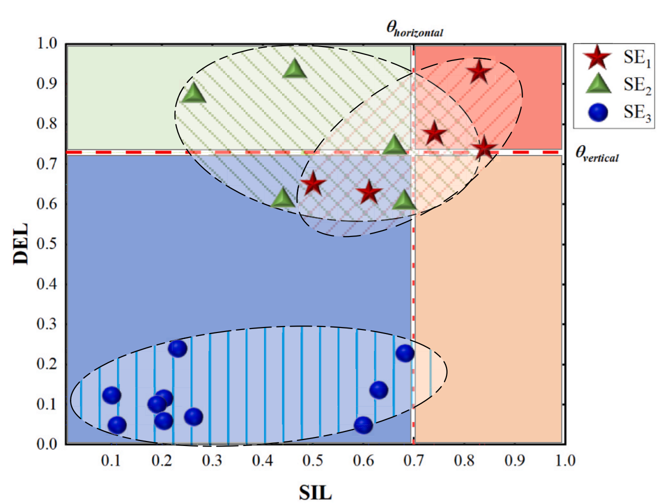

Fig. 12. The I-E matrix identification result of DMs.

crucial in the competitive NEV industry. Unlike fixed weight determination, this approach merges DMs' subjective preferences with algorithmically generated attribute weights. For instance, while algorithmically, data may prioritize range and battery efficiency, DMs may focus more on technological monopoly and advanced driver-assistance features. This approach balances AU and EU in weight assignment for DMs or entities, which is often overlooked in traditional methods. For example, input from an external consultant on emerging technologies can be weighted differently than an internal engineer's manufacturing expertise, increasing adaptability and transparency while providing stakeholders with clear, measurable justifications.

Phase 2: Apply Algorithm 3 to enforce a decentralized multipartite consensus mechanism.

Step 1: Consensus measurement. For each pair of DMs within a stakeholder entity, we calculate the initial consensus level using Definition 17. In this case, after careful consideration, the R&D department selects the accepted consensus levels as $\varpi_p = 0.97$.

Step 2: Decentralized multipartite consensus feedback mechanism. In this step, we firstly identify SE_1, SE_2 and SE_3 into different DMP. As the situation shown in Fig. 12, according to $\left|\left(\mathrm{IE}^{(H-L)} \cup \mathrm{IE}^{(H-H)}\right) \cap SE_1\right| = 3 > \frac{5}{3}$, $\left|\mathrm{IE}^{(L-H)} \cap SE_2\right| = 3 > \frac{5}{3}$, $\left|\mathrm{IE}^{(L-L)} \cap SE_3\right| = 10 \geq$

Table 7
The detailed calculation process of $dm_{1,1}$'s fine-grained DPRs on A_1

The initial evaluation on A_1 given by $dm_{1,1}$ with $H^{1,1}=\{(H_1)^{1,1},\cdots,(H_9)^{1,1}\}$								
A_l	$a_{1,v}$	$w^a_{1,v}$	$r^{1,1}_{1,v}$	$\widetilde{w}^{1,1}_{1,v}$	$H^{1,1}_{n,1,12}(a_{1,v})$	$H^{1,1}_{n,1,23}(a_{1,v})$	$H^{1,1}_{n,1,34}(a_{1,v})$	$H^{1,1}_{n,1,45}(a_{1,v})$
A_1	$a_{1,1}$	0.24	0.50	0.33	1	9	8	2
	$a_{1,2}$	0.16	0.30	0.19	3	5	6	5
	$a_{1,3}$	0.14	0.10	0.13	5	6	H	6
	$a_{1,4}$	0.13	0.60	0.25	6	H	5	6
	$a_{1,5}$	0.10	0.10	0.10	7	3	1	7
	$a_{1,6}$	0.08	0.08	0.08	H	5	H	H
	$a_{1,7}$	0.08	0.20	0.09	3	2	9	2
	$a_{1,8}$	0.07	0.10	0.08	4	1	7	1
The result of fine-grained DPRs on A_1 given by $dm_{1,1}$								
A_l	$s^{1,1}$		$(H_n)^{1,1}$		$f^{1,1}_{1,(12)}\left[(H_n)^{1,1}\right]$	$f^{1,1}_{1,(23)}\left[(H_n)^{1,1}\right]$	$f^{1,1}_{1,(34)}\left[(H_n)^{1,1}\right]$	$f^{1,1}_{1,(45)}\left[(H_n)^{1,1}\right]$
A_1	−1.00		$(H_1)^{1,1}$		0.264	0.062	0.077	0.062
	−0.75		$(H_2)^{1,1}$		0.000	0.071	0.000	0.335
	−0.50		$(H_3)^{1,1}$		0.223	0.077	0.000	0.000
	−0.25		$(H_4)^{1,1}$		0.062	0.000	0.000	0.000
	0.00		$(H_5)^{1,1}$		0.108	0.217	0.200	0.152
	0.25		$(H_6)^{1,1}$		0.200	0.108	0.152	0.308
	0.50		$(H_7)^{1,1}$		0.077	0.000	0.062	0.077
	0.75		$(H_8)^{1,1}$		0.000	0.000	0.264	0.000
	1.00		$(H_9)^{1,1}$		0.000	0.264	0.071	0.000
			$H^{1,1}$		0.065	0.200	0.173	0.065
Entropy					$E\left(d^{1,1}_{1,(12)}\right)$	$E\left(d^{1,1}_{1,(23)}\right)$	$E\left(d^{1,1}_{1,(34)}\right)$	$E\left(d^{1,1}_{1,(45)}\right)$
					0.169	0169	0.311	0.169
The normalized DPRs on A_1 transformed by fine-grained DPRs								
A_l	s^*		H^*_n		$d^{*1,1}_{1,(12)}(H^*_n)$	$d^{*1,1}_{1,(23)}(H^*_n)$	$d^{*1,1}_{1,(34)}(H^*_n)$	$d^{*1,1}_{1,(45)}(H^*_n)$
A_1	−1.00		H^*_1		0.264	0.097	0.077	0.229
	−0.50		H^*_2		0.254	0.113	0.000	0.168
	0.00		H^*_3		0.239	0.271	0.276	0.307
	0.50		H^*_4		0.177	0.054	0.270	0.232
	1.00		H^*_5		0.000	0.264	0.203	0.000
			H^*		0.065	0.200	0.173	0.065

Table 8
The coarse-grained DPRs given by $dm_{2,2}$ on A_1

A_l	s^C	H^C_n	$d^{*2,2}_{1,(12)}(H^C_n)$	$d^{*2,2}_{1,(23)}(H^C_n)$	$d^{*2,2}_{1,(34)}(H^C_n)$	$d^{*2,2}_{1,(45)}(H^C_n)$
A_1	−1.00	H^C_1	0	0.1	0	0
	−0.50	H^C_2	0.2	0.4	0	0
	0.00	H^C_3	0.7	0.4	0	0
	0.50	H^C_4	0.1	0.1	0.9	0
	1.00	H^C_5	0	0	0	1
		H^C	0	0	0.1	0
Entropy			$E\left(d^{2,2}_{1,(12)}\right)$	$E\left(d^{2,2}_{1,(23)}\right)$	$E\left(d^{2,2}_{1,(34)}\right)$	$E\left(d^{2,2}_{1,(45)}\right)$
			1.157	1.722	0.469	0

$\frac{10}{3}$ so that $SE_1 \in DMP^{MR}$, $SE_2 \in DMP^{MC}$, $SE_3 \in DMP^{NC}$. For SE_3, because there is no need to reach consensus in the entity which has low interest and expertise, the opinion of SE_3 $d^{*SE_3}_{(ij)}$ should be directly generated by Eq. (33). For SE_1, the consensus level $CL_1 = 0.877$ is firstly calculated by Definition 18. Since $CL_1 < \varpi_p$, we should apply **Model I** and generate optimized collective DPRs $\overline{d}^{*SE_1}_{(ij)}$. For SE_2, the consensus level $CL_2 = 0.873$ is firstly calculated by Definition 18. Since $CL_2 < \varpi_p$, we should apply **Model II** and generate optimized collective DPRs $\overline{d}^{*SE_2}_{(ij)}$. The final collective DPRs and the detailed optimal process of each entity are shown in Table 10.

Step 3: Decentralized multipartite selecting process. Based on Table 10, the collective DPRs are generated according to Eq. (49). Then, calculate its corresponding score value $S_C = \left(\left[S^{(C)-}_{ij}, S^{(C)+}_{ij}\right]\right)_{M\times M}$ and PD matrix $PD_C = \left(pd^C_{ij}\right)_{M\times M}$. The detailed calculating process and results are shown in Table 11. Therefore, the final alternatives ranking is $x_5 \succ x_4 \succ x_3 \succ x_2 \succ x_1$. The Tech-Smart SUV ($x_5$) is the optimal R&D alternative for its top score and highest PD in the comprehensive decision-making process. It strongly aligns with technology trends, consumer safety, connectivity, and innovation preferences.

5.2. Sensitivity analysis for two optimization models

This subsection will develop the sensitivity analysis conducted for models I and II. Figs. 13-15 show how different thresholds impact Model I and II outcomes in a GDM context.

Table 9
The reweighted results of individuals and entities.

SE_p	$dm_{p,k}$	$w^{dm}_{p,k}$	$E(dm_{p,k})$	$r^{dm}_{p,k}$	$\widetilde{w}^{dm}_{p,k}$	W^{SE}_p	$E(SE_p)$	R^{SE}_p	$\widetilde{W}^{SE}_p$
SE_1	$dm_{1,1}$	0.238	0.126	0.231	0.237	0.382	0.141	0.429	0.401
	$dm_{1,2}$	0.206	0.110	0.234	0.212				
	$dm_{1,3}$	0.198	0.128	0.231	0.204				
	$dm_{1,4}$	0.177	0.711	0.143	0.172				
	$dm_{1,5}$	0.180	0.593	0.161	0.177				
SE_2	$dm_{2,1}$	0.225	0.104	0.236	0.228	0.344	0.153	0.424	0.374
	$dm_{2,2}$	0.173	0.728	0.149	0.169				
	$dm_{2,3}$	0.231	0.146	0.230	0.231				
	$dm_{2,4}$	0.196	0.146	0.230	0.203				
	$dm_{2,5}$	0.174	0.684	0.155	0.171				
SE_3	$dm_{3,1}$	0.113	0.895	0.099	0.111	0.274	0.706	0.147	0.243
	$dm_{3,2}$	0.100	0.842	0.100	0.100				
	$dm_{3,3}$	0.094	0.761	0.101	0.095				
	$dm_{3,4}$	0.093	0.870	0.100	0.094				
	$dm_{3,5}$	0.099	0.873	0.099	0.099				
	$dm_{3,6}$	0.102	0.806	0.100	0.102				
	$dm_{3,7}$	0.095	0.862	0.100	0.096				
	$dm_{3,8}$	0.093	0.827	0.100	0.094				
	$dm_{3,9}$	0.098	0.861	0.100	0.098				
	$dm_{3,10}$	0.112	0.743	0.101	0.111				

Table 10
The collective DPRs of each stakeholder entity.

The result of collective DPRs by SE_1							**The optimal process of SE_1**	
s^*	−1	−0.5	0	0.5	1	–	Consensus level before optimization	0.877
H^*	H^*_1	H^*_2	H^*_3	H^*_4	H^*_5	H^*	Consensus level after optimization	0.970
$\overline{d}^{*SE_1}_{(12)}$	0.184	0.185	0.063	0.371	0.142	0.055	Number of Iterations	16
$\overline{d}^{*SE_1}_{(23)}$	0.175	0.131	0.158	0.319	0.149	0.067	Optimal objective function value	1.0564
$\overline{d}^{*SE_1}_{(34)}$	0.214	0.229	0.184	0.219	0.106	0.047	Decision variable	$\varrho_{1,1} = 0; \varrho_{1,2} = 1; \varrho_{1,3} = 0.15; \varrho_{1,4} = 0; \varrho_{1,5} = 1$
$\overline{d}^{*SE_1}_{(45)}$	0.247	0.178	0.094	0.316	0.108	0.057		
The result of collective DPRs by SE_2							**The optimal process of SE_2**	
s^*	−1	−0.5	0	0.5	1	–	Consensus level before optimization	0.873
H^*	H^*_1	H^*_2	H^*_3	H^*_4	H^*_5	H^*	Consensus level after optimization	0.970
$\overline{d}^{*SE_2}_{(12)}$	0.201	0.215	0.205	0.155	0.160	0.063	Number of Iterations	12
$\overline{d}^{*SE_2}_{(23)}$	0.232	0.217	0.140	0.158	0.170	0.084	Optimal objective function value	0.0731
$\overline{d}^{*SE_2}_{(34)}$	0.243	0.185	0.139	0.198	0.138	0.098	Decision variable	$\varrho_{1,1} = 0.57; \varrho_{1,2} = 0.49; \varrho_{1,3} = 0.50; \varrho_{1,4} = 0.49; \varrho_{1,5} = 0.49$
$\overline{d}^{*SE_2}_{(45)}$	0.247	0.172	0.137	0.157	0.179	0.108		
The result of collective DPRs by SE_3								
s^*	−1	−0.5	0	0.5	1	–		
H^*	H^*_1	H^*_2	H^*_3	H^*_4	H^*_5	H^*		
$d^{*SE_3}_{(12)}$	0.062	0.126	0.203	0.447	0.128	0.034		
$d^{*SE_3}_{(23)}$	0.155	0.246	0.224	0.281	0.051	0.044		
$d^{*SE_3}_{(34)}$	0.036	0.182	0.178	0.444	0.120	0.040		
$d^{*SE_3}_{(45)}$	0.049	0.219	0.234	0.351	0.113	0.034		

Table 11
The detailed calculation process of the decentralized multipartite selection process.

The final result of collective DPRs							**Score value**	**Possibility degree**
s^*	−1	−0.5	0	0.5	1	–	S_C	PD_C
H^*	H^*_1	H^*_2	H^*_3	H^*_4	H^*_5	H^*		
$\overline{d}^{*C}_{(12)}$	0.162	0.183	0.142	0.322	0.143	0.048	[-0.002, 0.098]	0
$\overline{d}^{*C}_{(23)}$	0.193	0.189	0.165	0.259	0.133	0.061	[-0.086, 0.036]	0.172
$\overline{d}^{*C}_{(34)}$	0.186	0.205	0.165	0.269	0.118	0.057	[-0.093, 0.021]	0.069
$\overline{d}^{*C}_{(45)}$	0.206	0.186	0.138	0.276	0.132	0.063	[-0.091, 0.035]	0.153

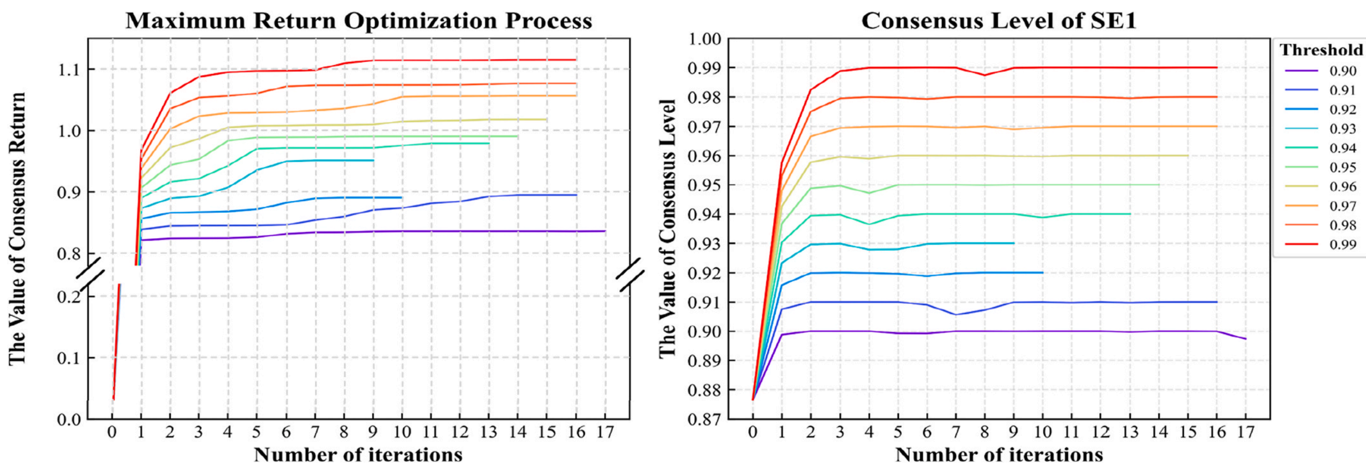

Fig. 13. Sensitivity analysis of maximum return optimization process.

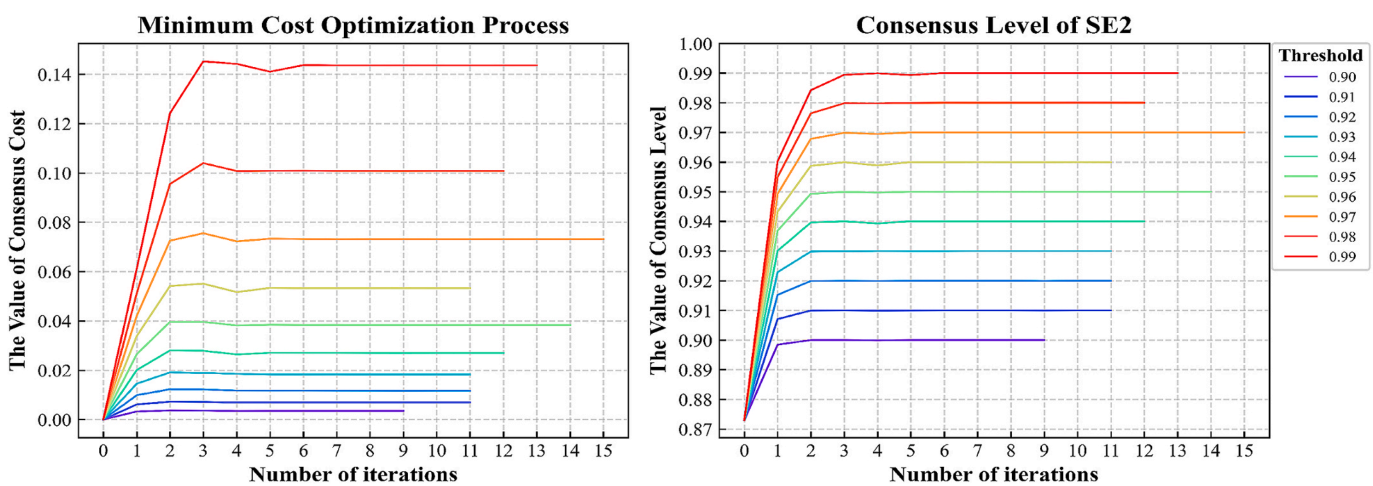

Fig. 14. Sensitivity analysis of minimum cost optimization process.

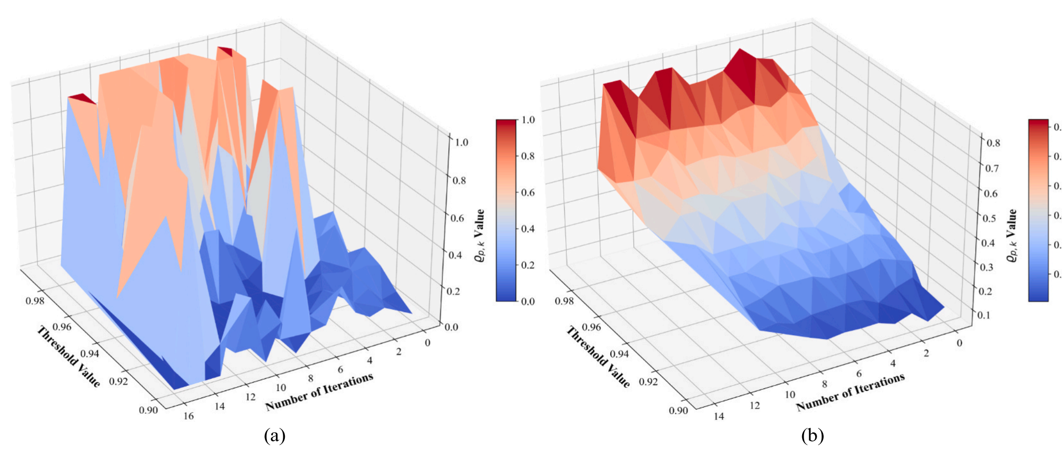

Fig. 15. History of decision variable solution under Model I and Model II.

Fig. 13 explores the impact of varying threshold levels on the maximum return optimization process and consensus level of SE_1. Here are some key observations. 1) For consensus return: the figure shows that higher threshold values generally lead to a higher value of consensus return. The return increases sharply at lower iteration counts, indicating rapid convergence at the beginning of the optimization process. As the threshold increases, the increase in consensus return becomes more gradual, suggesting that a higher threshold is required to reach a more stringent consensus. 2) For consensus level: it indicates that a higher threshold results in faster growth of the consensus level with iteration. The consensus level generally stabilizes after 5–10 iterations, indicating that most optimization benefit is gained early. A lower threshold (e.g., 0.90) reaches a stable consensus level faster than a higher threshold (e.g., 0.99), which takes more iterations to stabilize.

Fig. 14 illustrates the minimum cost optimization process and its related impact on the consensus level of SE_2 across varying threshold values. Observations from it include: 1) For consensus cost, it reveals that a lower threshold value is associated with a quicker stabilization of consensus cost, whereas a higher threshold extends the number of iterations required before reaching consensus. This indicates that a tighter consensus threshold initially elevates the cost, possibly due to more significant adjustments needed to meet stricter consensus criteria. 2) For consensus level: similar to the findings in maximum return, the higher threshold initially enlarges the consensus level quickly, yet it gradually stabilizes over successive iterations. Notably, consensus levels are swift to reach stability for thresholds such as 0.90 and 0.91, suggesting that less stringent thresholds facilitate easier consensus among DMs.

Fig. 15 provides a visual representation of the decision variable ($\varrho_{p,k}$) under multiple iterations and different threshold levels in the two optimization models. Here are the insights derived from the analysis: 1) **Model I** exhibits more variability in $\varrho_{p,k}$ values across different threshold settings. The decision variable fluctuates significantly, indicating its sensitivity to the threshold parameter. 2) **Model II** displays a smoother transition in $\varrho_{p,k}$ values, with a gradual increase as iterations progress. The smoother surface suggests that this model is less sensitive to the changes in threshold values and might offer more robust performance under varying conditions.

Overall, the sensitivity analysis highlights varying consensus threshold levels' impact on performance outcomes. The consensus threshold determines the strictness of the required agreement among DMs and plays a crucial role in the update of the decision variable $\rho_{(p,k)}$. These observations underline the trade-offs between the two models: while a higher threshold in Model I can yield a more substantial consensus at the expense of increased volatility and longer convergence times, Model II provides a more stable and robust performance in terms of cost efficiency. This sensitivity analysis thus offers critical guidance for parameter tuning, ensuring that the decision-making process can be optimally adjusted based on the desired balance between consensus strength and computational stability.

5.3. Qualitative comparisons with other methods

5.3.1. Qualitative comparisons with several GDM problems focusing on UGC

In this section, we conduct a comparative analysis of the proposed decentralized multipartite feedback mechanism with other GDM approaches that concentrate on utilizing UGC. To illustrate the distinctions and commonalities with other GDM methods, Table 12 compares based on characteristics such as data source handling, weight determination method, decision model, and application area.

5.3.2. Qualitative comparisons with other attribute discovery methods

Various attribute discovery methods exist, ranging from purely qualitative, expert-driven frameworks to classical topic-modeling

Table 12
Comparison with other GDM models focusing on UGC.

Reference	Characteristics	Data sources	Weight determination	Decision model	Application
(Wu et al., 2023)	Large-scale alternatives Multiple online platforms	Collect online platform data (*movie rating*) from *IMDb*, *MTime*, and *Douban.*	Information entropy of time series The number of evaluations	Multivariate time-series-based decision-making method	Rank movies among a set of large-scale alternatives
(Liu et al., 2023)	UGC Interactive criteria Risk preference	Crawl online medical platform UGC (*reviews* for psychologists) posted on *haodf.com*	Entropy-based method Whitening method	Integrate sentiment analysis method and MCDM method	Rank psychologists from haodf.com
(Ji et al., 2023a)	User demands and user satisfaction Community detection	Crawl online P2P accommodation platform data (*reviews*) from *Airbnb*	A minimal variance approach Consensus-based assignment of weight	Integrate sentiment analysis method and large-scale group consensus-based method.	Evaluate user satisfaction with sharing accommodation.
(Qin and Zeng, 2022)	Aggregate multiple classifiers using ER theory Stochastic multi-criteria acceptability analysis-PROMETHEE method	Crawl online data (*reviews*) from the *JingDong Mall website*	A TextRank algorithm for objectively determining the weight	Integrate the MCDM method based on sentiment analysis and stochastic dominance rules	Rank products based on online reviews in China's e-commerce
(Darko et al., 2023)	Convert huge online consumer reviews into PLTSsLatent Dirichlet Allocation topic modeling approach	Crawl online consumer information (*reviews*) from the *Google Play Store*	A probabilistic linguistic indifference threshold-based attribute ratio analysis	Integrate text mining analytics with uncertain MADM	Evaluate and rank m-payment services
(He et al., 2022)	Interval-valued linguistic distribution assessment (ILDA)Extend ER algorithm to ILDA environment	Crawl online consumer data (*reviews*) from *JingDong Mall website*	–	Integrate incomplete textural analysis with the MADA framework	Compare and rank mobile phones
(Yang et al., 2021)	Focus on the online discussion system or social democratic systemCase-based reasoning algorithm for consensus decision-making support (CDMS)	Create some cases using the online data collected from *COLLAGREE* online discussion forums	–	A machine learning-based framework for CDMS in crowd-scale deliberation	Facilitate online discussion toward smoothing a consensus decision
(Xu et al., 2021)	The location of collection and delivery points (CDPs) optimizationQuantitative analysis of the relationship between customer service level and retailers' benefit	A real-world data set (*users' basic information and their activity logs*) provided by the *Ali IJCAI*	–	Integrate data mining models and facility location models	Determine CDP locations for online retailers
(Wu and Liao, 2021)	Psychological intensity based on Weber-Fechner's lawUtility-based translation method	Collect all data (*quantitative parameters and online reviews*) from *Amazon.com*.	–	Model the personalized cognition of customers on both quantitative and qualitative information.	Television selection from Amazon.com
(Guo et al., 2020)	A more interpretable model than the traditional recommender systemPairwise comparisons within an aggregation-disaggregation paradigm	Available data (a set of online *reviews* and *ratings*) provided by product manager	Weight constraints	A data-driven MCDA approach to integrate online information, such as explicit and implicit feedback from consumers	Assist product manager in analyzing the consumer's preferences for smartphones.
This research	UXO attribute system generationDecentralized multipartite consensus feedback mechanism	An automobile review platform (*pcauto.com.cn*)	Weight determination and reweighting function design	Decentralized multipartite consensus mechanism for MAGDM	R&D alternative selection for NEV

Table 13
Comparison with other GDM models focusing on UGC.

	The proposed method	MR	MC	Liu's method (Liu et al., 2024)
DMs scale	$SE = [5,5,10]$	20	20	20
Algorithm time cost	**1.6313**	**57.4889**	**31.0915**	**10.0274**
Number of Iterations	28	35	32	31
Final consensus level	0.970	0.970	0.970	0.981
The final alternatives ranking	$x_5 \succ x_4 \succ x_3 \succ x_2 \succ x_1$	$x_5 \succ x_4 \succ x_2 \succ x_3 \succ x_1$	$x_5 \succ x_4 \succ x_3 \succ x_2 \succ x_1$	$x_5 \succ x_4 \succ x_3 \succ x_2 \succ x_1$

approaches. Unlike manual curation, which relies on limited insights from domain experts, our proposed method integrates large-scale UGC through advanced SBER and a novel SSRcos metric. This approach offers several key advantages. i) Comprehensive coverage: We capture a broader spectrum of user concerns by processing extensive corpora, ensuring that emerging preferences are not overlooked. ii) Adaptive refinement: The method can be periodically re-run to adapt to shifts in user sentiment, providing an advantage over static, expert-crafted index systems that risk becoming obsolete. iii) Balanced emphasis: a data-driven weighting scheme (A-TF-IDF) highlights frequent and distinctive attributes, aligning them more effectively with real-world user priorities than simple frequency counts. Consequently, our technique is a powerful, scalable tool for constructing attribute systems, positioning it favorably relative to purely qualitative or conventional statistical approaches.

5.4. Quantitative comparisons with other methods

To quantitatively validate the advantages of our decentralized multipartite consensus model, we conducted a comprehensive comparison experiment against three existing methods, namely MR, MC, and Liu's method (Liu et al., 2024). Table 13 presents the results under a uniform stakeholder configuration ($SE = [5,5,10]$, i.e., 20 decision makers) and the same consensus threshold. Although all methods reached a similarly high level of agreement, with final consensus levels at or near 0.97, the proposed method converged in the fewest iterations while achieving the lowest algorithm time cost. Such efficiency is crucial for real-world large-scale group decision-making, where time-to-consensus often determines the final recommendations' feasibility. Notably, Liu's method attained a marginally higher consensus (0.981) but required more computational effort (10.0274) than our approach (1.6313). This trade-off highlights the flexibility of the proposed model, which offers a balanced compromise between rapid convergence and consensus quality. Consequently, these findings underscore our framework's reliability, scalability, and cost-effectiveness in handling complex decision scenarios derived from UGC.

6. Conclusion

In the realm of MAGDM, this research introduces a data-driven approach, focusing on UGC to extract and systematize user experience attributes. This approach distinctively contrasts with traditional methods by prioritizing user-centric data, enabling the creation of a more refined and accurate attribute system. This research integrates a decentralized multipartite consensus mechanism tailored to diverse stakeholder groups, facilitating robust consensus aligned with DMs' varying expertise and interest levels. Building upon a data-driven approach in MAGDM, this study introduces three key advancements: 1) An innovative UXO attribute system that leverages NLP techniques and advanced statistical methods to enhance the granularity and relevance of UGC data analysis. 2) An I-E responsive multi-granularity decision mechanism that effectively aligns decision granularity with diverse stakeholder expertise enhances organizational decision-making. 3) A decentralized multipartite feedback mechanism that ensures inclusive, robust, and adaptable consensus among stakeholders with varying interests and expertise levels, suitable for complex decision environments.

Integrating a refined attribute system and robust consensus mechanism contributes to more reliable organizational decision-making. This approach not only aligns decisions with users' genuine preferences and expectations but also ensures that these decisions are finely tuned to the dynamic demands of the market. Businesses can tap into consumer insights by focusing on UGC, enabling a more user-centric approach that enhances customer satisfaction and loyalty. Furthermore, organizations can foster greater inclusivity and equity in decision-making by accommodating a wide range of stakeholder views through a flexible and multipartite consensus mechanism. This improves the quality and acceptance of decisions and enhances organizational agility, allowing businesses to respond more swiftly and effectively to market changes and new opportunities.

In future research, we aim to refine the integration of our attribute system and consensus mechanism with real-time analytics, enhancing responsiveness to dynamic market conditions and user feedback. This would involve deploying machine learning algorithms to predict changes in user preferences and adapting the decision-making process accordingly. Additionally, exploring the model's scalability across different industries and cultural contexts could provide valuable insights into its universal applicability and potential for customization based on specific market needs.

Declaration of competing interest

The authors declare that they have no known competing financial interests or personal relationships that could have appeared to influence the work reported in this paper.

Acknowledgments

This research is supported by the National Natural Science Foundation of China under the Grant No.72471069, 72471137, 72371093, 72271077, 72371095, and Projects of International Cooperation and Exchanges NSFC (W2411063).

Appendix A

Table A1
Abbreviations mentioned in the main text.

Abbreviation	Denotation	Abbreviation	Denotation
AU	aleatoric uncertainty	AR	adjustment return
A-TF-IDF	attribute-based TF-IDF	BD	Belief Distribution
BOE	bodies of evidence	C-H	Calinski-Harabasz
CRP	consensus reaching process	CDPR	complete distributed preference relation
DPR	distributed preference relation	DM	decision maker
D-B	Davies-Bouldin	DEL	domain expertise level
DMP	decision-making participative party	EU	epistemic uncertainty
KDI	knowledge dissemination index	I-E	interest-expertise
IR	Identification Return	IVS	interest valuation score
MAGDM	multi-attribute group decision making	NEV	new energy vehicle
NLP	natural language processing	PTS	peer-reviewed trust score
PLPR	probabilistic linguistic preference relation	PLM	pre-trained language models
R&D	research and development	ROI	return on involvement
SEL	stakeholder engagement level	SBERT	sentence-BERT
SNA	social network analysis	STS	semantic textual similarity
SC	silhouette coefficient	SIL	stakeholder interest level
T-SNA	trust social network analysis	UXO	user experience-oriented
UGC	user-generated content	TF-IDF	term frequency–inverse document frequency
UMAP	Uniform Manifold Approximation and Projection	HDBSCAN	hierarchical density-based spatial clustering of applications with noise

Table A2
Symbols in the main text.

Symbol	Description
$X = \{x_1, \cdots, x_m, \cdots, x_M\}(M \geq 2)$	The set of alternatives
$A = \{A_1, \cdots, A_l, \cdots, A_L\}(L \geq 2)$	The upper layer attributes set
$a = \left\{ \begin{matrix} a_{1,1}, \cdots, a_{1,n_1}; \cdots; \\ a_{l,1}, \cdots, a_{l,n_l}; \cdots; \\ a_{L,1}, \cdots, a_{L,n_L} \end{matrix} \right\}$	The lower layer attributes set
$W^A = \{W_l^A \mid l = 1, \cdots, L\}$	The weights of L upper layer attributes
$w^a = \left\{ \begin{matrix} w^a_{1,1}, \cdots, w^a_{1,n_1}; \cdots; \\ w^a_{l,1}, \cdots, w^a_{l,n_l}; \cdots; \\ w^a_{L,1}, \cdots, w^a_{L,n_l} \end{matrix} \right\}$	The weights of lower layer attributes
$H = \{H_1, \cdots, H_n \cdots, H_N\}$	The set of evaluation grades
$SE = \{SE_1, \cdots, SE_p, \cdots, SE_P\}(SE \geq 2)$	The set of stakeholder entities
$SE_p = \{dm_{p,1}, \cdots, dm_{p,k}, \cdots, dm_{p,n_p}\}$	The set of DMs in the p_{th} stakeholder entity SE_p
W_p^{SE}, $w_{p,k}^{dm}$	The relative weight of SE_p, $dm_{p,k}$
$D_{p,k} = (d_{ij}^{p,k})_{M\times M}, d_{ij}^{p,k} = \left\{ \left(H_n, d_{ij}^{p,k}(H_n)\right), n = 1, \cdots, N; \left(H, d_{ij}^{p,k}(H)\right) \right\}$	The DPR matrix given by the $dm_{p,k}$
$S_{p,k} = \left(\left[S_{ij}^{(p,k)-}, S_{ij}^{(p,k)+}\right]\right)_{M\times M}$	The score matrix of $dm_{p,k}$
$PD_{p,k} = \left(pd_{ij}^{p,k}\right)_{M\times M}$	The possibility degree matrix of $dm_{p,k}$
$diss\left(d_{ij}^{p,k}, d_{ij}^{p,g}\right)$	The preference dissimilarity measure of $dm_{p,k}$ and $dm_{q,g}$
$\lambda_{kg} = (t_{kg}, d_{kg})$	The trust relationship from dm_k to dm_g
$TS = [ts_{kg}]_{n_p\times n_p}$	The trust score matrix of SE_p
$U = [u_1, u_2, \cdots, u_T] \in \mathbb{R}^{1\times T}$, $V = [v_1, v_2, \cdots, v_T] \in \mathbb{R}^{1\times T}$	Sentence embedding vectors
$SSRcos(U, V)$	The segment soft relative cosine similarity
$\mathrm{A} = \{\alpha_1, \alpha_2, \cdots, \alpha_N\}$, $\mathrm{\beta} = \{\beta_1, \beta_2, \cdots, \beta_N\}$	The high-dimensional dataset and low-dimensional dataset
$CE = \sum_i \sum_j \left[p_{ij} log\left(\frac{p_{ij}}{q_{ij}}\right) + \left(1 - p_{ij}\right) log\left(\frac{1 - p_{ij}}{1 - q_{ij}}\right) \right]$	The objective function of UMAP
$d_{\mathrm{mreach}\text{-}\sigma}\left(\beta_i, \beta_j\right)$	The mutual reachability distance between two points β_i and β_j
$TF-IDF_{\mathrm{Attribute}}\left(t_{l,i}, A_l\right), W_{t_{l,i}}$	Attribute-based TF-IDF and the relative weight of $t_{l,i}$
$\theta_{horizontal}, \theta_{vertical}$	Two thresholds of Interest-Expertise stakeholder matrix
$IE^{H-H}, IE^{L-H}, IE^{L-L}, IE^{H-L}$	I-E (High-High/ Low-High/ Low-Low/ High-Low)
$SIL(dm_{p,k})$	Stakeholder interest level
$ROI(dm_{p,k}), SEL(dm_{p,k}), IVS(dm_{p,k})$	Return on Involvement/Stakeholder Engagement Levels/ Interest Valuation Score
$DEL(dm_{p,k})$	DM’s domain expertise
$PTS(dm_{p,k})$, $\mathrm{KDI}\ (dm_{p,k})$	Peer-reviewed trust score/Knowledge Dissemination Index
$H^{p,k} = \left\{(H_1)^{p,k}, \cdots, (H_n)^{p,k}, \cdots, (H_N)^{p,k}\right\}$	The fine-grained frame of discernment by $dm_{p,k}$
$d_{l,(ij)}^{p,k} = \left\{ \left((H_n)^{p,k}, f_{l,(ij)}^{p,k}\left[(H_n)^{p,k}\right]\right), n = 1, \cdots, N; \left(H^{p,k}, f_{l,(ij)}^{p,k}\left(H^{p,k}\right)\right) \right\}$	The fine-grained DPR given by $dm_{p,k}$ for compare x_i to x_j
$\widetilde{w}_{l,v}^{p,k}, w_{l,v}^{a}, r_{l,v}^{p,k}$	Adjust weight/ the original weight/ the relative importance
$H^C = \{H_1^C, \cdots, H_n^C, \cdots, H_N^C\}$	The coarse-grained frame of discernment by $dm_{p,k}$

(continued on next page)

Table A2 (*continued*)

Symbol	Description
$d^{p,k}_{l,(ij)} = \left\{ \left(H^C_n, c^{p,k}_{l,(ij)}(H^C_n) \right), n = 1, \cdots, N'; \left(H^C, c^{p,k}_{l,(ij)}(H^C) \right) \right\}$	The coarse-grained DPR given by $dm_{p,k}$ for compare x_i to x_j
$\mathfrak{B}^{p,k}_{l,(ij)}$	The bodies of evidence
$E\left(d^{p,k}_{l,(ij)}\right), E\left(d^{p,k}_{l}\right), E\left(d^{p,k}_{(ij)}\right), E(dm_{p,k})$	The belief entropy of $d^{p,k}_{l,(ij)}$
$\widetilde{W}^{p,k}_l, W^A_l, R^{p,k}_l$	The adjusted weights/ the initial weight/ the reliability of $dm_{p,k}$
$\widetilde{w}^{dm}_{p,k}, w^{dm}_{p,k}, r^{dm}_{p,k}$	The reweighted relative/ the original relative weight/ the reliability score of $dm_{p,k}$
$\widetilde{W}^{SE}_p, W^{SE}_p, R^{SE}_p$	The reweighted relative/ the original relative weight/ the reliability score of SE_p
$d^{*p,k}_{l,(ij)} = \left\{ \left(H^*_n, d^{*p,k}_{l,(ij)}(H^*_n) \right), n = 1, \cdots, N; \left(H^*, d^{*p,k}_{l,(ij)}(H^*) \right) \right\}$	The normalized DPR matrix
CL_{kg}, CL_p	Consensus level between two DMs or stakeholder entity
$DMP^{NC}, DMP^{MR}, DMP^{MC}$	Non-Consensual/Maximum Return/Minimum Cost Participants
$IR_{p,k}, AR_{p,k}$	The Identification Return/ Adjustment Return of $dm_{p,k}$
$r_{p,k}, c_{p,k}$	The unit reward/consensus cost of $dm_{p,k}$
UR_p	The total return of SE_p
$CC_{p,k}$	The consensus cost of $dm_{p,k}$

Appendix B. Supplementary data

Supplementary data to this article can be found online at https://doi.org/10.1016/j.eswa.2025.127917.

Data availability

Data will be made available on request.

References

Bai, W., Zhang, C., Zhai, Y., & Sangaiah, A. K. (2024). A robust incomplete large-scale group decision-making model for metaverse metro operations and maintenance. *Applied Soft Computing, 156*, Article 111472.

Bezdek, J. C., Spillman, B., & Spillman, R. (1978). A fuzzy relation space for group decision theory. *Fuzzy Sets and Systems, 1*, 255–268.

Chen, H., Shao, L., Zhou, L., & Liu, J. (2024). Maximum consensus model with individual tolerance and mixed DEA prospect cross-efficiency for multi-attribute group decision-making. *Applied Soft Computing, 158*, Article 111572.

Cheng, D., Cheng, F., Zhou, Z., & Wu, Y. (2020). Reaching a minimum adjustment consensus in social network group decision-making. *Information Fusion, 59*, 30–43.

Darko, A. P., Liang, D., Xu, Z., Agbodah, K., & Obiora, S. (2023). A novel multi-attribute decision-making for ranking mobile payment services using online consumer reviews. *Expert Systems with Applications, 213*, Article 119262.

Dong, Y., Zhang, H., & Herrera-Viedma, E. (2016). Consensus reaching model in the complex and dynamic MAGDM problem. *Knowledge-Based Systems, 106*, 206–219.

Fu, C., Chang, W., Xue, M., & Yang, S. (2019). Multiple criteria group decision making with belief distributions and distributed preference relations. *European Journal of Operational Research, 273*, 623–633.

Fu, C., Xu, D., & Yang, S. (2016). Distributed preference relations for multiple attribute decision analysis. *Journal of the Operational Research Society, 67*, 457–473.

Guo, M., Liao, X., Liu, J., & Zhang, Q. (2020). Consumer preference analysis: A data-driven multiple criteria approach integrating online information. *Omega, 96*, Article 102074.

Han, Y., Ji, Y., & Qu, S. (2022). A robust minimum-cost consensus model with uncertain aggregation weights based on data-driven method. *IEEE Transactions on Computational Social Systems, 9*, 1167–1184.

He, S., Wang, Y., Pan, X., & Chin, K.-S. (2022). Decision analysis framework based on incomplete online textual reviews. *Information Sciences, 584*, 701–718.

Ji, F., Cao, Q., Li, H., Fujita, H., Liang, C., & Wu, J. (2023a). An online reviews-driven large-scale group decision making approach for evaluating user satisfaction of sharing accommodation. *Expert Systems with Applications, 213*, Article 118875.

Ji, F., Wu, J., Chiclana, F., Wang, S., Fujita, H., & Herrera-Viedma, E. (2023b). The overlapping community-driven feedback mechanism to support consensus in social network group decision making. *IEEE Transactions on Fuzzy Systems, 31*, 3025–3039.

Kumar, K., & Chen, S.-M. (2022). Multiple attribute group decision making based on advanced linguistic intuitionistic fuzzy weighted averaging aggregation operator of linguistic intuitionistic fuzzy numbers. *Information Sciences, 587*, 813–824.

Lan, Z., Chen, M., Goodman, S., Gimpel, K., Sharma, P., & Soricut, R. (2019). ALBERT: A Lite BERT for Self-supervised Learning of Language Representations. *Presented at the International Conference on Learning Representations*.

Landauer, T. K., Foltz, P. W., & Laham, D. (1998). An introduction to latent semantic analysis. *Discourse Processes, 25*, 259–284.

Li, Y., Kou, G., Li, G., & Peng, Y. (2022). Consensus reaching process in large-scale group decision making based on bounded confidence and social network. *European Journal of Operational Research, 303*, 790–802.

Liu, F., Liao, H., & Al-Barakati, A. (2023). Physician selection based on user-generated content considering interactive criteria and risk preferences of patients. *Omega, 115*, Article 102784.

Liu, P., Li, Y., & Wang, P. (2023). Social trust-driven consensus reaching model for multiattribute group decision making: Exploring social trust network completeness. *IEEE Transactions on Fuzzy Systems, 31*, 3040–3054.

Liu, W., Wu, Y., Chen, X., & Chiclana, F. (2024). Managing heterogeneous preferences and multiple consensus behaviors with self-confidence in large-scale group decision making. *Information Fusion, 107*, Article 102289.

Ma, Z., Zhu, J., & Chen, Y. (2020). A probabilistic linguistic group decision-making method from a reliability perspective based on evidential reasoning. *IEEE Transactions on Systems, Man, and Cybernetics: Systems, 50*, 2421–2435.

Qin, J., & Zeng, M. (2022). An integrated method for product ranking through online reviews based on evidential reasoning theory and stochastic dominance. *Information Sciences, 612*, 37–61.

Reimers, N., Gurevych, I., 2019. Sentence-BERT: Sentence Embeddings using Siamese BERT-Networks. In: *EMNLP-IJCNLP 2019*. Presented at the EMNLP-IJCNLP 2019, Association for Computational Linguistics, Hong Kong, China, pp. 3982–3992.

Tang, G., Fu, R., Seiti, H., Chiclana, F., & Liu, P. (2025). A novel bi-objective R-mathematical programming method for risk group decision making. *Information Fusion, 118*, Article 102902.

Tang, G., Gu, X., Chiclana, F., Liu, P., & Yin, K. (2023a). A multi-objective q-rung orthopair fuzzy programming approach to heterogeneous group decision making. *Information Sciences, 645*, Article 119343.

Tang, G., Long, J., Gu, X., Chiclana, F., Liu, P., & Wang, F. (2022). Interval type-2 fuzzy programming method for risky multicriteria decision-making with heterogeneous relationship. *Information Sciences, 584*, 184–211.

Tang, G., Zhang, X., Zhu, B., Seiti, H., Chiclana, F., & Liu, P. (2023b). A mathematical programming method based on prospect theory for online physician selection under an R-set environment. *Information Fusion, 93*, 441–468.

Tang, M., Zhou, X., Liao, H., Xu, J., Fujita, H., & Herrera, F. (2019). Ordinal consensus measure with objective threshold for heterogeneous large-scale group decision making. *Knowledge-Based Systems, 180*, 62–74.

Wang, B., & Liang, J. (2020). A novel preference measure for multi-granularity probabilistic linguistic term sets and its applications in large-scale group decision-making. *International Journal of Fuzzy Systems, 22*, 2350–2368.

Wei, J., Qu, S., Wang, Q., Luan, D., & Zhao, X. (2023). The novel data-driven robust maximum expert mixed integer consensus models under multirole's opinions uncertainty by considering noncooperators. *IEEE Transactions on Computational Social Systems, 10*, 3454–3470.

Wu, J., Jin, Y., Zhou, M., Cao, M., & Liu, Y. (2022). A group consensus decision making based sustainable supplier selection method by combing DEMATEL and VIKOR. *Journal of Intelligent & Fuzzy Systems, 42*, 2595–2613.

Wu, J., Xiong, R., & Chiclana, F. (2016). Uninorm trust propagation and aggregation methods for group decision making in social network with four tuple information. *Knowledge-Based Systems, 96*, 29–39.

Wu, X., & Liao, H. (2021). Modeling personalized cognition of customers in online shopping. *Omega, 104*, Article 102471.

Wu, X., Liao, H., & Tang, M. (2023). Decision making towards large-scale alternatives from multiple online platforms by a multivariate time-series-based method. *Expert Systems with Applications, 212*, Article 118838.

Xing, Y., Cao, M., Liu, Y., Zhou, M., & Wu, J. (2022). A Choquet integral based interval Type-2 trapezoidal fuzzy multiple attribute group decision making for Sustainable Supplier Selection. *Computers & Industrial Engineering, 165*, Article 107935.

Xu, X., Du, Z., & Chen, X. (2015). Consensus model for multi-criteria large-group emergency decision making considering non-cooperative behaviors and minority opinions. *Decision Support Systems, 79*, 150–160.
Xu, X., Shen, Y., Chen, W. (Amanda), Gong, Y., & Wang, H. (2021). Data-driven decision and analytics of collection and delivery point location problems for online retailers. *Omega, 100*, Article 102280.
Xue, M., Fu, C., & Yang, S. (2021). Dynamic expert reliability based feedback mechanism in consensus reaching process with distributed preference relations. *Group Decision and Negotiation, 30*, 341–375.
Yang, C., Gu, W., Ito, T., & Yang, X. (2021). Machine learning-based consensus decision-making support for crowd-scale deliberation. *Applied Intelligence, 51*, 4762–4773.
Yang, J., & Xu, D. (2013). Evidential reasoning rule for evidence combination. *Artificial Intelligence, 205*, 1–29.
Zhang, B., Liang, H., Zhang, G., & Xu, Y. (2018). Minimum deviation ordinal consensus reaching in GDM with heterogeneous preference structures. *Applied Soft Computing, 67*, 658–676.
Zhang, G., Dong, Y., & Xu, Y. (2014). Consistency and consensus measures for linguistic preference relations based on distribution assessments. *Information Fusion, 17*, 46–55.
Zhang, H., Dong, Y., & Herrera-Viedma, E. (2018). Consensus building for the heterogeneous large-scale GDM with the individual concerns and satisfactions. *IEEE Transactions on Fuzzy Systems, 26*, 884–898.
Zhang, H., Wang, F., Dong, Y., Chiclana, F., & Herrera-Viedma, E. (2022). Social trust driven consensus reaching model with a minimum adjustment feedback mechanism considering assessments-modifications willingness. *IEEE Transactions on Fuzzy Systems, 30*, 2019–2031.
Zhang, Y., Xu, Z., Wang, H., & Liao, H. (2016). Consistency-based risk assessment with probabilistic linguistic preference relation. *Applied Soft Computing, 49*, 817–833.
Zhang, Z., Li, Z., & Gao, Y. (2021). Consensus reaching for group decision making with multi-granular unbalanced linguistic information: A bounded confidence and minimum adjustment-based approach. *Information Fusion, 74*, 96–110.
Zhao, S., Zhang, T., Hu, M., Chang, W., & You, F. (2022). AP-BERT: Enhanced pre-trained model through average pooling. *Applied Intelligence, 52*, 15929–15937.
Zhou, M., Guan, Z., Chen, Y., Zhou, Z., Wu, J., & Herrera-Viedma, E. (2022a). Consistency and consensus reaching process for group decision making based on complete interval distributed preference relations under social network analysis. *Information Fusion, 88*, 126–145.
Zhou, M., Qiao, Y., Yang, J., Zhou, Y., Liu, X.-B., & Wu, J. (2022b). A three-level consensus model for large-scale multi-attribute group decision analysis based on distributed preference relations under social network analysis. *Expert Systems with Applications, 204*, Article 117603.
Zhou, M., Zheng, Y., Chen, Y., Cheng, B., Herrera-Viedma, E., & Wu, J. (2023). A large-scale group consensus reaching approach considering self-confidence with two-tuple linguistic trust/distrust relationship and its application in life cycle sustainability assessment. *Information Fusion, 94*, 181–199.
Zhou, M., Zhou, Y., Yang, J., & Wu, J. (2024). A generalized belief dissimilarity measure based on weighted conflict belief and distance metric and its application in multi-source data fusion. *Fuzzy Sets and Systems, 475*, Article 108719.
Zhou, Y.-J., Zhou, M., Liu, X.-B., Cheng, B.-Y., & Herrera-Viedma, E. (2022c). Consensus reaching mechanism with parallel dynamic feedback strategy for large-scale group decision making under social network analysis. *Computer & Industrial Engineering, 174*, Article 108818.